ISSN:2149-1909

THE JOURNAL OF NEUROBEHAVIORAL SCIENCES

(J Neuro Behav Sci)

Volume: 9

Issue: 3 (December)

Year: 2022

NÖRODAVRANIŞ BİLİMLERİ DERGİSİ

Wolters Kluwer

JNBS Publication of Uskudar University

Neurosurgery

Psychology,
Psychiatry, Neurology

Full-Fledged
General Hospital

Private 7 / 24 Psychiatric
Intensive Care Unit

1A Operating Rooms

NPAMATEM
Addiction Center

Fully-Equipped
Intensive Care Unit

Personalized
Pharmacogenetic
Treatment

Child Psychiatry,
Neurology, Neurosurgery

Neuromodulation
Center

Üsküdar University
Science Partner

NP İSTANBUL Hospital

We are inspired by the
brain to achieve excellence

npistanbulbrainhospital nphospital.pac nphospital www.npistanbul.com/en

Saray Mah. Ahmet Tevfik İleri Cad. No:18, 34768 Ümraniye / İstanbul TURKEY
T: 00905312945555 | 00905386358998

Üsküdar University Science Partner

ISSN:2149-1909

The Journal of Neurobehavioral Sciences

Editorial Board

Volume: 9 Issue Number: 3 (December) Year: 2022

Period
Published 3 times a year (March-August-December) distributed free of charge. Print Date / August 2022

IT / Technical Service
Hakan Özdemir

**The Journal of Neurobehavioral Sciences (JNBS) is a peer-reviewed open-access neuroscience journal without any publication fees.
**JNBS published both electronically and hard copy printed forms 3 times a year by Uskudar University.
**JNBS accepts articles written in English language.

ABOUT THIS JOURNAL

Publication Policy

The Journal of Neurobehavioral Sciences (J Neuro Behav Sci) is a peer-reviewed open-access neuroscience journal without any publication fees. All editorial costs are sponsored by the Üsküdar University Publications and the Foundation of Human Values and Mental Health. Each issue of the Journal of Neurobehavioral Sciences is specially commissioned, and provides an overview of important areas of neuroscience from the molecular to the behavioral levels, delivering original articles, editorials, reviews and communications from leading researchers in that field. JNBS is published electronically and in the printed form 3 times a year by Uskudar University. The official language of JNBS is English. The average time from delivery to first decision is less than 30 days. Accepted articles are published online on average on 40 working days prior to printing, and articles are published in print at 3-6 months after acceptance. Please see our Guide for Authors for information on article submission. If you require any further information or help, please email us (jnbs@uskudar.edu.tr)

Aims & Scope

JNBS (J. Neuro. Behav. Sci) is a comprehensive scientific journal in the field of behavioral sciences. It covers many disciplines and systems (eg neurophysiological, neuroscience systems) with behavioral (eg cognitive neuroscience) and clinical aspects of molecules (eg molecular neuroscience, biochemistry), and computational methods in health.

The journal covers all areas of neuroscience with an emphasis on psychiatry and psychology as long as the target is to describe the neural mechanisms underlying normal or pathological behavior. Pre-clinical and clinical studies are equally acceptable for publication. In this context; the articles and treatment results of computational modeling methods of psychiatric and neurological disorders are also covered by the journal.

JNBS emphasis on psychiatric and neurological disorders. However, studies on normal human behavior are also considered. Animal studies and technical notes must have a clear relevance and applicability to human diseases. Case Reports including current neurological therapies or diagnostic methods are generally covered by JNBS.

Besides; The scope of JNBS is not limited to the abovementioned cases, and publications produced from the interdisciplinary studies established in the following fields and with the behavioral sciences are included in the studies that can be published in JNBS.

• Cognitive neuroscience
• Psychology
• Psychiatric and neurological disorders
• Neurophysiology
• System neuroscience
• Molecular neuroscience
• Computational Neuroscience
• Neuromodulation, Neurolinguistic, Neuromarketing
• Biochemistry
• Computational and simulation methods and interdisciplinary applications in medicine
• Artificial Intelligence (AI) and interdisciplinary applications in medicine
• Brain imaging
• In vivo monitoring of electrical and biochemical activities of the brain
• Molecular Biology
• Genetics
• Bioinformatics
• Psychiatric Nursing

INSTRUCTIONS FOR AUTHORS

Prior to submission, please carefully read and follow the submission guidelines entailed below. Manuscripts that do not conform to the submission guidelines may be returned without review.

Submission

Submit manuscripts electronically (.doc format with including all figures inside) via the online submission system of our website (https://review.jow.medknow.com/jnbs).

Assoc. Prof. Dr. Turker Tekin Erguzel, Ph.D Co-Editor, Journal of Neurobehavioral Sciences Department of Psychology

Uskudar University Altunizade Mh., Haluk Türksoy Sk No: 14, İstanbul-Turkey

General correspondence may be directed to the Editor's Office.

In addition to postal addresses and telephone numbers, please supply electronic mail addresses and fax numbers, if available, for potential use by the editorial and production offices.

Masked Reviews

Masked reviews are optional and must be specifically requested in the cover letter accompanying the submission. For masked reviews, the manuscript must include a separate title page with the authors' names and affiliations, and these ought not to appear anywhere else in the manuscript. Footnotes that identify the authors must be typed on a separate page. Make every effort to see that the manuscript itself contains no clues to authors' identities. If your manuscript was mask reviewed, please ensure that the final version for production includes a byline and full author note for typesetting.

Similarity Rate: The similarity of the submitted articles with the Ithenticate program is determined. The similarity rate should be below 20%.

Types of Articles: Brief Reports, commentaries, case reports and minireviews must not exceed 4000 words in overall length. This limit includes all aspects of the manuscript (title page, abstract, text, references, tables, author notes and footnotes, appendices, figure captions) except figures.

Brief Reports also may include a maximum of two figures.

For Brief Reports, the length limits are exact and must be strictly followed. Regular Articles typically should not exceed 6000 words in overall length (excluding figures).

Reviews are published within regular issues of the JNBS and typically should not exceed.

10000 words (excluding figures)

Cover Letters

All cover letters must contain the following: A statement that

the material is original —if findings from the dataset have been previously published or are in other submitted articles, please include the following information:

*Is the present study a new analysis of previously analyzed data? If yes, please describe differences in analytic approach.

*Are some of the data used in the present study being analyzed for the first time? If yes, please identify data (constructs) that were not included in previously published or submitted manuscripts.

*Are there published or submitted papers from this data set that address related questions? If yes, please provide the citations, and describe the degree of overlap and the unique contributions of your submitted manuscript.

*The full postal and email address of the corresponding author; *The complete telephone and fax numbers of the same;

*The proposed category under which the manuscript was submitted;

*A statement that the authors complied with APA ethical standards in the treatment of their participants and that the work was approved by the relevant Institutional

Review Board(s).

*Whether or not the manuscript has been or is posted on a web site;

*That APA style (Publication Manual, 6th edition) has been followed;

*The disclosure of any conflicts of interest with regard to the submitted work;

*A request for masked review, if desired, along with a statement ensuring that the manuscript was prepared in accordance with the guidelines above.

*Authors should also specify the overall word length of the manuscript (including all aspects of the manuscript, except figures) and indicate the number of tables, figures, and supplemental materials that are included.

Manuscript Preparation

Prepare manuscripts according to the Publication Manual of the American Psychological Association (6th edition).

Review APA's Checklist for Manuscript Submission before submitting your article. Double-space all copy. Other formatting instructions, as well as instructions on preparing tables, figures, references, metrics, and abstracts, appear in the Manual.

Below are additional instructions regarding the preparation of display equations and tables.

Display Equations

We strongly encourage you to use MathType (third-party software) or Equation

Editor 3.0 (built into pre-2007 versions of word) to construct your equations, rather than the equation support that is built into Word 2007 and Word 2010. Equations composed with the built-in Word 2007/Word 2010 equation support are converted to low-resolution graphics when they enter the production process and must be rekeyed by the typesetter, which may introduce errors.

To construct your equations with MathType or Equation Editor 3.0:

Go to the Text section of the Insert tab and select Object.

Select MathType or Equation Editor 3.0 in the drop-down menu.

If you have an equation that has already been produced using Microsoft Word 2007 or 2010 and you have access to the full version of MathType 6.5 or later, you can convert this equation to MathType by clicking on MathType Insert Equation. Copy the equation from Microsoft Word and paste it into the MathType box. Verify that your equation is correct, click File, and then click Update. Your equation has now been inserted into your Word file as a MathType Equation.

Use Equation Editor 3.0 or MathType only for equations or for formulas that cannot be produced as word text using the Times or Symbol font.

Tables

Use Word's Insert Table function when you create tables. Using spaces or tabs in your table will create problems when the table is typeset and may result in errors.

Abstract and Keywords

All manuscripts must include an English abstract containing a maximum of 250 words typed on a separate page. (It should contain headings such as Background, Aims and Objectives, Materials and Methods, Results, Conclusion etc.) After the abstract, please supply up to five keywords or brief phrases.

References:

Vancouver is a numbered referencing style used in JNBS.

Citations to someone else's work in the text, indicated by the use of a number. A sequentially numbered reference list at the end of the document providing full details of the corresponding in-text reference.

General rules of in-text citation:

- A number is allocated to a source in the order in which it is cited in the text. If the source is referred to again, the same number is used.
- Use Arabic numerals (1,2,3,4,5,6,7,8,9).
- Either square [ ] or curved brackets ( ) can be used as long as it is consistent.
- In the publication, source numbers are indicated in parentheses or as superscripts at the end of the sentence - name - in which the source is used.
- If the sources with consecutive numbers are to be displayed at the same time, the first and last numbers are separated with "-"

According to some estimates, the prevalence of ADHD has increased up to 30% in the last 20 years.[1]
S variant is associated with the lower transcriptional activity of the promoter when compared to the L variant.[4,7-9,11]

The Reference Section:

• Journal Article:

Russell FD, Coppell AL, Davenport AP. In vitro enzymatic processing of radiolabelled big ET-1 in human kidney as a food ingredient. Biochem Pharmacol 1998;55(5):697-701. doi: 10.1016/s0006-2952(97)00515-7.

Gonen, M. Planning for subgroup analysis: a case study of treatmentmarker interaction in metastatic colorectal cancer. Controlled Clinical Trials 2003;24 : 355-363. doi: 10.1016/s0197-2456(03)00006-0.

• Authored Book:

Lodish H, Baltimore D, Berk A, Zipursky SL, Matsudaira P, Darnell J. Molecular cell biology. 3rd ed. New York: Scientific American; 1995.

Millares M, editor. Applied drug information: strategies for information management. Vancouver: Applied Therapeutics, Inc.; 1998.

Figures

Graphics files are welcome if supplied as Tiff, EPS, or PowerPoint files. Multipanel figures (i.e., figures with parts labeled a, b, c, d, etc.) should be assembled into one file.

The minimum line weight for line art is 0.5 point for optimal printing

PUBLICATION ETHICS AND PUBLICATION MALPRACTICE STATEMENT (ETHICAL GUIDELINES FOR PUBLICATION)

The publication of an article in the peer-reviewed journal JNBS is an essential building block in the development of a coherent and respected network of knowledge. It is a direct reflection of the quality of the work of the authors and the institutions that support them. Peer-reviewed articles support and embody the scientific method. It is therefore important to agree upon standards of expected ethical behaviour for all parties involved in the act of publishing: the author, the journal editor, the peer reviewer, the publisher and the society of society-owned or sponsored journals.

Uskudar University, as publisher of the journal, takes its duties of guardianship over all stages of publishing extremely seriously and we recognise our ethical and other responsibilities.

We are committed to ensuring that advertising, reprint or other commercial revenue has no impact or influence on editorial decisions. In addition, Editorial Board will assist in communications with other journals and/or publishers where this is useful to editors. Finally, we are working closely with other publishers and industry associations to set standards for best practices on ethical matters, errors and retractions - and are prepared to provide specialized legal review and counsel if necessary.

Duties of authors

(These guidelines are based on existing COPE's Best Practice Guidelines for Journal Editors.)

Reporting standards

Authors of reports of original research should present an accurate account of the work performed as well as an objective discussion of its significance. Underlying data should be represented accurately in the paper. A paper should contain sufficient detail and references to permit others to replicate the work. Fraudulent or knowingly inaccurate statements constitute unethical behavior and are unacceptable. Review and professional publication articles should also be accurate and objective, and editorial 'opinion' works should be clearly identified as such.

Authors are required to state in writing that they have complied with the Declaration of Helsinki Research Ethics in the treatment of their sample, human or animal, or to describe the details of treatment.

Data access and retention

Authors may be asked to provide the raw data in connection with a paper for editorial review, and should be prepared to provide public access to such data (consistent with the ALPSP-STM Statement on Data and Databases), if practicable, and should in any event be prepared to retain such data for a reasonable time after publication.

Originality and plagiarism

The authors should ensure that they have written entirely original works, and if the authors have used the work and/or words of others, that this has been appropriately cited or quoted.

Plagiarism takes many forms, from 'passing off' another's paper as the author's own paper, to copying or paraphrasing substantial parts of another's paper (without attribution), to claiming results from research conducted by others. Plagiarism in all its forms constitutes unethical publishing behavior and is unacceptable.

Multiple, redundant or concurrent publication

An author should not in general publish manuscripts describing essentially the same research in more than one journal or primary publication. Submitting the same manuscript to more than one journal concurrently constitutes unethical publishing behavior and is unacceptable.

In general, an author should not submit for consideration in another journal a previously published paper. Publication of some kinds of articles (e.g. clinical guidelines, translations) in more than one journal is sometimes justifiable, provided certain conditions are met. The authors and editors of the journals concerned must agree to the secondary publication, which must reflect the same data and interpretation of the primary document. The primary reference must be cited in the secondary publication. Further detail on acceptable forms of secondary publication can be found at www. icmje.org.

Acknowledgement of sources

Proper acknowledgment of the work of others must always be given. Authors should cite publications that have been influential in determining the nature of the reported work. Information obtained privately, as in conversation, correspondence, or discussion with third parties, must not be used or reported without explicit, written permission from the source. Information obtained in the course of confidential services, such as refereeing manuscripts or grant applications, must not be used without the explicit written permission of the author of the work involved in these services.

Authorship of the paper

Authorship should be limited to those who have made a significant contribution to the conception, design, execution, or interpretation of the reported study. All those who have made significant contributions should be listed as co-authors. Where there are others who have participated in certain substantive aspects of the research project, they should be acknowledged or listed as contributors.

The corresponding author should ensure that all appropriate coauthors and no inappropriate coauthors are included on the paper, and that all co-authors have seen and approved the final version of the paper and have agreed to its submission for publication.

Hazards and human or animal subjects

If the work involves chemicals, procedures or equipment that have any unusual hazards inherent in their use, the author must clearly identify these in the manuscript. If the work involves the use of animal or human subjects, the author should ensure that the manuscript contains a statement that all procedures were performed in compliance with relevant laws and institutional guidelines and that the appropriate institutional committee(s) has approved them. Authors should include a statement in the manuscript that informed consent was obtained for experimentation with human subjects. The privacy rights of human subjects must always be observed.

Disclosure and conflicts of interest

All authors should disclose in their manuscript any financial or other substantive conflict of interest that might be construed to influence the results or interpretation of their manuscript. All sources of financial support for the project should be disclosed.

Examples of potential conflicts of interest which should be disclosed include employment, consultancies, stock ownership, honoraria, paid expert testimony, patent applications/registrations, and grants or other funding. Potential conflicts of interest should be disclosed at the earliest stage possible.

Fundamental errors in published works

When an author discovers a significant error or inaccuracy in his/her own published work, it is the author's obligation to promptly notify the journal editor or publisher and cooperate with the editor to retract or correct the paper. If the editor or the publisher learns from a third party that a published work contains a significant error, it is the obligation of the author to promptly retract or correct the paper or provide evidence to the editor of the correctness of the original paper.

Duties of editors

(These guidelines are based on existing COPE's Best Practice Guidelines for Journal Editors.)

Publication decisions

The editor of a peer-reviewed journal is responsible for deciding which of the articles submitted to the journal should be published, often working in conjunction with the relevant society (for societyowned or sponsored journals). The validation of the work in question and its importance to researchers and readers must always drive such decisions. The editor may be guided by the policies of the journal's editorial board and constrained by such legal requirements as shall then be in force regarding libel, copyright infringement and plagiarism. The editor may confer with other editors or reviewers (or society officers) in making this decision.

Fair play

An editor should evaluate manuscripts for their intellectual content without regard to race, gender, sexual orientation, religious belief, ethnic origin, citizenship, or political philosophy of the authors.

Confidentiality

The editor and any editorial staff must not disclose any information about a submitted manuscript to anyone other than the corresponding author, reviewers, potential reviewers, other editorial advisers, and the publisher, as appropriate.

Disclosure and conflicts of interest

Unpublished materials disclosed in a submitted manuscript must not be used in an editor's own research without the express written consent of the author.

Privileged information or ideas obtained through peer review must be kept confidential and not used for personal advantage.

Editors should recuse themselves (i.e. should ask a co-editor, associate editor or other member of the editorial board instead to review and consider) from considering manuscripts in which they have conflicts of interest resulting from competitive, collaborative, or other relationships or connections with any of the authors, companies, or (possibly) institutions connected to the papers.

Editors should require all contributors to disclose relevant competing interests and publish corrections if competing interests are revealed after publication. If needed, other appropriate action should be taken, such as the publication of a retraction or expression of concern.

It should be ensured that the peer-review process for sponsored supplements is the same as that used for the main journal. Items in sponsored supplements should be accepted solely on the basis of academic merit and interest to readers and not be influenced by commercial considerations.

Non-peer reviewed sections of their journal should be clearly identified.

Involvement and cooperation in investigations

An editor should take reasonably responsive measures when ethical complaints have been presented concerning a submitted manuscript or published paper, in conjunction with the publisher (or society). Such measures will generally include contacting the author of the manuscript or paper and giving due consideration of the respective complaint or claims made, but may also include further communications to the relevant institutions and research bodies, and if the complaint is upheld, the publication of a correction, retraction, expression of concern, or other note, as may be relevant. Every reported act of unethical publishing behavior must be looked into, even if it is discovered years after publication.

Duties of reviewers

(These guidelines are based on existing COPE's Best Practice Guidelines for Journal Editors.)

Contribution to editorial decisions

Peer review assists the editor in making editorial decisions and through the editorial communications with the author may also assist the author in improving the paper. Peer review is an essential component of formal scholarly communication, and lies at the heart of the scientific method. JNBS shares the view of many that all scholars who wish to contribute to publications have an obligation to do a fair share of reviewing.

Promptness

Any selected referee who feels unqualified to review the research reported in a manuscript or knows that its prompt review will be impossible should notify the editor and excuse himself from the review process.

Confidentiality

Any manuscripts received for review must be treated as confidential documents. They must not be shown to or discussed with others except as authorized by the editor.

Standards of objectivity

Reviews should be conducted objectively. Personal criticism of the author is inappropriate. Referees should express their views clearly with supporting arguments.

Acknowledgement of sources

Reviewers should identify relevant published work that has not been cited by the authors. Any statement that an observation, derivation, or argument had been previously reported should be accompanied by the relevant citation. A reviewer should also call to the editor's attention any substantial similarity or overlap between the manuscript under consideration and any other published paper of which they have personal knowledge.

Disclosure and conflict of interest

Unpublished materials disclosed in a submitted manuscript must not be used in a reviewer's own research without the express written consent of the author. Privileged information or ideas obtained through peer review must be kept confidential and not used for personal advantage. Reviewers should not consider manuscripts in which they have conflicts of interest resulting from competitive, collaborative, or other relationships or connections with any of the authors, companies, or institutions connected to the papers.

The Journal of Neurobehavioral Sciences

Volume 9 ¦ Issue 3 ¦ September-December 2022

Contents

ORIGINAL ARTICLES

Original Article

Examination of the Relationship between Depressive Mood Level and Attentional Bias

Nazende Ceren Öksüz Özdemir[1]

[1]*Dogus University, İstanbul, Turkey*

Abstract

Summary: Attention is defined as the cognitive process to detect a particular internal or external stimulus, and maintaining focus are closely related to mood. The orientation of the attention resource (Attention allocation) is shaped by the mood of the person. Focusing more on negative and threatening stimuli than neutral and/or positive stimuli in the outside world is called "Attentional Bias". This article emphasizes that attentional bias is linked with the level of depressive mood state, between a low level of depressive mood and a high level of depression. **Aim:** This research aimed to examine if there is an attentional bias toward negative stimuli among individuals with depressive symptoms. **Materials and Methods:** The Hamilton Depression Rating Scale and the Point Locating Task were administered to the participants. The research consists of a sample of 90 undergraduate and graduate students selected by random sampling method. **Results:** Based on the research findings, there is a positive and significant relationship between the level of depression and attentional orientation. The result of the study indicated that there is a significant negative relationship between depression scores and attentional orientation. When the attentional bias of the participants was examined according to their depression levels, it was found that the attentional bias of the participants with moderate depression symptoms was significantly higher than those without depression symptoms. **Conclusion:** These results indicated that relationship between attentional bias and depression level. Further studies are needed to examine depression levels and attentional bias levels in a larger sample size.

Keywords: *Attention, attentional bias, cognitive processing, depression, dysthymia, mood disorders*

Introduction

Attention includes expressions, including the individual's perception and interpretation of an existing item or event, the organism's methods of obtaining information, and the development of problem-solving skills.[1] As a widely known expression, attention is defined as certain conscious reactions created for the stimuli perceived by the sensory system and the orientation of the mental process.[2]

The concept of attention is a subject emphasized in many fields, including psychology, education, and sociology. Since not all stimuli in the outside world can be processed by the human brain, certain stimuli are passed through a filter.[3] While the important and necessary stimuli are selected and included in the information processing, some of the stimuli that are not important, negative, or currently useless are generally ignored.[4]

Attention is automatic or controlled reaction with certain levels of effort, selective based on the individual-target relationship, divided and focused based on the number of stimuli present in the environment. In addition, attention is divided as sustained attention according to the duration of focus.[5] It is known that the organism selects the stimuli that are important for it due to its limited capacity, and the elimination of the stimuli that are not important could be maintained through selective attention. The fact that the speed of perceiving important stimuli takes a shorter time compared to other stimuli is defined as attentional bias, which is a concept related to selective attention. Attentional bias is the tendency to prioritize the perception and interpretation of stimuli that are important to the organism.[6]

How to cite this article: Öksüz Özdemir NC. Examination of the relationship between depressive mood level and attentional bias. J Neurobehav Sci 2022;9:83-9.

Ethics committee approval: The ethics committee approval has been obtained from Dogus University Committee. (No:E-42435178-050.06.04-36367/Date:14.11.22).

Received : 23-09-2022
Accepted : 15-11-2022
Published : 29-12-2022

Orcid
Nazende Ceren Öksüz Özdemir {ORCID: 0000-0002-5961-1688}

Address for correspondence:
Ms. Nazende Ceren Öksüz Özdemir,
Dogus University, Istanbul, Turkey.
E-mail: nazendeoksuz@gmail.com

Access this article online

Website: www.jnbsjournal.com

DOI: 10.4103/jnbs.jnbs_25_22

Quick Response Code:

For instance, important names, numbers, messages with emotional content, stimuli associated with pathologies including anxiety disorder and depression, and stimuli that may pose a threat to the individual may lead to the development of attentional bias.[7-10]

Mood disorders are characterized by intense unhappiness. Mood disorders are among the most common mental illnesses worldwide. In general, depression manifests itself with a decrease in self-confidence that can last for years, the lack of pleasure and interest in work and life, hopelessness, and social isolation. Certain factors, including daily life stressors, traumas, and the environment, increase the likelihood of a person having depression symptoms. However, despite the presence of the triggering environmental factors, the severity of depression symptoms can differ. The diagnostic and statistical manual of mental disorders (DSM 5) has a wide variety of subdimensions specific to the diagnosis of depressive disorders. These include disruptive mood dysregulation disorder, major depressive disorder, dysthymia, premenstrual dysphoric disorder, substance-related depressive disorder, depressive disorder resulting from medical disorders, and undifferentiated depressive disorder. However, the most prevalent type is a major depressive disorder. According to DSM 5, the symptoms of major depression are depressed mood, decreased interest and desire, appetite disorders, sleep disorders, slowed psychomotor activity or restless mood, fatigue, guilt, feeling of worthlessness, attention disorders, and suicidality.[11] While some of the symptoms may be the result of sadness in the face of any situation, some of them may be a symptom of depression in a more complicated way. At this point, symptoms can be categorized according to the severity of the condition. For instance, psychomotor agitation, suicidal thoughts, psychotic thoughts, the feeling of worthlessness, and significant functional impairment are determinant findings for depression. On the other hand, sadness, loss of appetite, insomnia, difficulty with concentrating, and fatigue can be included as a symptom of depression if they are observed with more severe symptoms mentioned above.[12]

When the relationship between attention and depression is examined, people with depression usually pay attention to information that is related or consistent with their negative cognitive schemas and then easily remember them. Among depressive individuals, the attention source is directed more toward negative stimuli and positive stimuli are ignored, which is called "Attentional Bias."[13,14] According to a review study examining the relationship between attentional bias and depression, it was found that depressed individuals had more biased attention to negative stimuli toward themselves and their environment.[15]

The speed of perception for an emotional situation can provide information regarding attentional bias. In a study Suslow, Junghanns, and Arolt. in 2001, it was revealed that patients diagnosed with depression react more slowly to positive emotions. When the reactions shown to negative facial expressions are examined in the same study, there is no significant difference between patients with depression and individuals without a diagnosis of depression. It was also found that patients with depression showed a relatively slower response to positive facial expressions. Emotional expressions were more intense in negative situations due to attentional bias among individuals with depressive symptoms. Therefore, for depressive individuals, attentional bias slows down the process of focusing on positive situations and events.[16]

Cognitive symptoms in depressed individuals are usually reduced cognitive flexibility and inadequacy of thought content. People with depressive symptoms often have slower information processing speeds. Patients with depression may have difficulty with maintaining their daily routines. Furthermore, they may be very busy with their work, family, money, and health, but their preoccupations are mostly pessimistic and hopeless.[17]

The study by Taşpınar and Pakyürek in 2020, it was found that the more emotional encoding of personal memories of individuals may affect their attention to stimuli. It was also noted in the study that diagnosis duration, depression subtype, drug or substance use, and which subitems they have in DSM-V diagnostic criteria should be determined when considering their level of attention. In the same study, it was also thought that there might be differences between those who meet the criteria for difficulty in concentration and those who do not when elaborating on the dysfunctions in attention. Researchers also indicated that the presence of people with different psychiatric diagnoses along with depression might prevent a meaningful conclusion from being drawn between the severe depression group and the moderate depression group. Therefore, it can be understood that there is a need for studies examining the relationship between attention and depressive symptoms.[11]

Individuals with depressive symptoms tend to pay more attention to negative information than to positive information. Selective attentional bias in information processing is very important in terms of its continuance and repetition. In a study by Baert, Raedt, Schact, and Koster (2010), the effects of bias modification on depressed patients were examined. According to the results of the research, it was observed that as the severity of depression increased, attentional bias increased among the patients. According to the results obtained in terms of attentional bias modification, it was concluded that moderate and severe depressive symptoms increased after training.[18] In another study conducted with images for examining attentional biases of depressed individuals toward interpersonal aggression, it was found that depressive individuals show biased attention toward aggressive pictures.[19] conducted a study with participants with high levels of trait anxiety and state anxiety. The results showed that female participants had attentional biases toward

angry faces, whereas it was observed that male participants showed an attentional bias toward cheerful faces.[20]

In another study, in which emotions were expressed with facial expressions, it was hypothesized that depressed individuals pay more attention to angry faces. Based on the findings, when depressed individuals are compared with individuals without a history of depression, there is a stronger attention for angry faces among individuals with depressive symptoms compared to the healthy control group.[21]

In another study by Bodenschatz, Scopinceva, Rub, Suslow (2019), it was hypothesized that individuals with the major depressive disorder had an attentional bias towards negative emotions, and it was pointed out that the reasons could be related to early maladaptive life events, namely childhood traumas. Study findings indicated that negative attentional bias of depressed individuals is related to childhood traumas and that negative attentional bias increases according to the severity of childhood traumas. In addition, as depression increases, attentional bias also increases in this study.[22]

In another study by Boyacıoğlu and Aktaş, it was found that as the symptoms of depression progress, people put their negative memories and life events at the center of their lives. As the level of depression increases, the individual tends to have more negative feelings and thoughts.[23] Another study was conducted to turn attentional bias among adolescents with depressive symptoms. Based on the findings, depression level increases while attentional bias increases among adolescents.[24]

In another study examining whether attention can be controlled with attentional bias modification in major depression or not, it was found that the level of depression and attentional bias toward negative emotions and thoughts significantly correlated.[25] However, Krings, Heeren, Fontain, Blairty has an experiment with face expressing different emotions with individualc with a diagnosis of major depressive disorder, indivivualrs with depressive symptoms even without a major depressive disorder diagnosis, and individuals without any symptoms of depression. The results of the study indicate that there is no positive or negative attentional bias among depressed individuals.[26]

Elgersma, Koster, Vugteveen, Hoekzema, Pennix, Bckting (2019), conducted retrospective scans of depressed patients over a 4-year periond and noticed that the same negative attentional bias was not present in each depressive episode. According to this study, there is no continuation of attentional bias, which includes the same positive or negative emotions, in severe depression. Based on the findings, as the severity of depression increases, attentional bias may increase, may not change, or may decrease. This situation can be explained by individual differences.

In light of the literature related to the relationship between depressive symptoms and attentional bias, it can be considered that there is a positive and significant relationship between attentional bias and depression. In line with this study, when the literature is examined, it is aimed to examine the relationship between depression and attentional bias to examine the relationship between these two concepts in detail. In this direction, research questions will be listed as follows:

Is there a significant relationship between depression and attentional bias?

Do depressed individuals have increased attentional bias toward negative emotions?

Materials and Methods

The ethics committee approval has been obtained from Dogus University Committee. (No:E-42435178-050.06.04-36367/Date:14.11.22).

Sample

The age range of the research sample was 20–45 years. Participants are university students at Yeditepe University, Sabancı University, and Gedik University. In order to eliminate the confounding effect that may occur due to the psychiatric comorbidity of people with mild depressive symptoms, a clinical interview was conducted, and the brief symptom inventory (BSI) was applied. Participants with the possibility of psychiatric comorbidity based on clinical evaluation and BSI results were excluded from the study. The sample was chosen by random sampling method, and quantitative data collection methods were used in the study.

Point locating task was applied to measure attentional orientation, which includes the calculation of the reaction rate to the positive stimulus.

The Hamilton Depression Rating Scale was used to measure the symptoms of depression. The sample consisted of people with a score between 3 and 17.

Participants who used psychiatric drugs and received psychotherapy in the last 2 months, had comorbid psychopathology, had organic brain disease, were in grief, wore glasses and had visual impairments, and did not have computer skills were excluded from the study.

The ethics committee approval has been obtained from Dogus University Committee.

Measurement and materials

Demographic information form

Demographic information form was created as a form, in which the characteristics of the participants, including age, gender, marital status, occupation, education level, and eye health were recorded.

Brief symptom inventory

BSI was developed by Derogatis in 1992 and adapted into Turkish by Hisli Şahin and Durak in 1994. The BSI,

consisting of one additional scale and nine subscales, is a 53-item self-report inventory. BSI evaluates the psychological symptoms of a total of 10 symptom groups and the level of strain related to these symptoms. Three global indexes are obtained from the inventory. These indices are: "Symptom Total Index," "Symptom Severity Index," and "Global Severity Index."[28]

Cronbach reliability values were determined by alpha analysis; item total coefficient was in the range of 0.21–0.78, and the reliability coefficient was found as 0.97. BSI has five subscales, including negative self, hostility, somatization, anxiety, and depression. Higher scores indicate an increase in the relevant subscale and the highest total score that can be obtained is 212.[27]

Hamilton depression rating scale

Hamilton Depression Rating Scale was developed in 1960 and was adapted by Akdemir *et al*. in 1996. The 17-item scale aims to measure the symptom pattern and severity of depression. The level of sexual desire, difficulty in falling asleep, waking up in the middle of the night, waking up early in the morning, weight loss, somatic symptoms, and poor insight are scored between 0 and 2, while the remaining items are scored individually. A range of 0–7 points indicates the absence of depression. A score of 8–15 indicates mild depression, a score of 16–28 indicates moderate depression, and a score of 29 and above indicates severe depression.

Point locating task

MacLeod, Mathews, and Tata formulated this task in 1986 to assess attentional bias. This task has been widely used in attentional bias studies since then. The Point Locator Task begins with an "X." After this sign disappears from the screen after 1000 ms, a word pair appears on the left and right of the screen at equal intervals (13 cm). This pair of words that appear will disappear after 500 ms and a dot appears on the left or right side. The dot remains on the screen until the participant presses the keyboard key in the direction it is associated with. Thus, it is determined that the participant reacts more quickly to the point after which word content and this reaction speed is recorded. In this configuration, both the region where the dot appears, and the distribution of word contents are equalized to control the confounding effect that may occur depending on the direction.

In this study, the Point Locating Task, which was developed for the measurement of attentional bias, was developed with the "OpenSesame 3.3.9" program. OpenSesame is a software and an algorithm used in psychology, neuroscience, and experimental economics. During the application with the software, words with negative and positive content were added to this interface one by one.

Procedure

The research was conducted in an online environment, preliminary information was given to the participants to meet the technical conditions. A list of 120 applicants was evaluated prior to the application. Participants who could not meet the technical requirements were not included in the study. A clinical interview and BSI were conducted with people who met the inclusion criteria. The Point Locating Task and the Hamilton Depression Scale were applied to the participants who met the inclusion criteria. The sample consists of 90 participants. The application was conducted with the shared screen with Teamviewer. For the results not to be affected by the screen size of the computers, it is provided to use laptops in the 15–16-inch range. Besides, it has been confirmed that the internet speed is in the ideal range of 16–35 Mbps. In case of Internet disconnection, the internet provider of the mobile phone was used during the application. The participant's distance with the screen was fixed at 60 cm, and it was ensured that the participant did not change his direction or distance during the application. The researcher was present online throughout the process.

Results

The frequency distributions of the participants' socio-demographic variables are given [Table 1]. In the study, which included 90 participants, 57.8% (52 people) were female and 42.2% (38 people) were men. According to education level, undergraduate graduates are 68.9% (62 people) and postgraduate graduates are 31.1% (28 people). According to the marital status variable, the rate of single people is 53.3% (48 people) and married people are 46.7% (42 people).

Kolmogorov–Smirnov and Shapiro–Wilk values given in Table 2 are $P < 0.05$, it is seen that the data do not show

Table 1:Frequency distributions of sociodemographic variables

Sociodemographic variables	Groups	Frequency (%)
Gender	Female	52 (57.8)
	Male	38 (42.2)
Level of education	Undergraduate	62 (68.9)
	Graduate	28 (31.1)
Marital status	Single	48 (53.3)
	Married	42 (46.7)
	Total	90 (100.0)

Table 2: Normality test findings

	Kolmogorov–Smirnov			Shapiro–Wilk		
	Statistics	df	*P*	Statistics	df	*P*
Hamilton Depression Scale	0.167	90	<0.001	0.903	90	<0.001
Attentional orientation	0.217	90	<0.001	0.891	90	<0.001

a normal distribution. In this case, nonparametric measures were preferred, and depression and attentional orientation scores were examined.

Spearman correlation findings of the relationship between Depression and Attention Direction Scores of the participants in Table 3, a strong, negative and significant relationship was found between depression (r_s = −0.911; $P < 0.001$) and attentional orientation.

Results of the Whitney *U* test comparison of depression and attention orientation scores by gender are given in Table 4.

Mann–Whitney *U* test findings in Table 4, the mean rank of Hamilton Depression Scale scores was found to be significantly higher in female participants ($\bar{x}$ *Rank* = 50.56) than male participants ($\bar{x}$ *Rank* = 38.58) (u = 725,000; P = 0.031; $P < 0.05$). Attention Orientation Scores do not differ significantly by gender.

Kruskal–Wallis test findings regarding the differentiation of the participants' attentional orientation scores according to their depression levels in Table 5, it was determined that attentional orientation differed significantly according to the depression level (χ^2 = 67,749; $P < 0.001$). According to the results of the dual group Mann–Whitney *U* test, which was used to determine the source of the difference, the participants without depression symptoms had the highest mean scores on attention orientation. In addition, the mean scores of the participants with moderate depression symptoms were found to be the lowest.

Table 3: Spearman correlation findings

Hamilton Depression Scale	Attentional orientation
r_s	−0.911**
P	<0.001
n	90

**P<0.01

Table 4: Mann–Whitney *U*-test findings for comparison of depression and attention orientation scores by gender

Dependent variables	Gender	n	$\bar{x}$ order	Rank sum	U	P
Hamilton Depression Scale	Woman	52	50.56	2629.00	725,000	0.031*
	Male	38	38.58	1466.00		
Attention orientation	Woman	52	41.37	2151.00	773.000	0.078
	Male	38	51.16	1944.00		

*P<0.05

Conclusion and Discussion

The main purpose of this study, which assumes that there is a significant correlation between the depression levels of individuals and their attentional bias toward negative events and situations, is to examine the relationship between depression and attentional bias. According to the results obtained from the study for this objective, as the level of depression increases, the attentional bias also increases. There is a strong and significant negative relationship between depression and attentional orientation. The results indicated that functional attentional functions were lower among individuals who reported higher scores in depression. The analysis of the obtained data was provided, and the findings were evaluated within the scope of the literature. It was seen that the findings obtained because of the evaluations were especially supported by the literature. Depression causes the individual's information processing to shift to the negative aspects of situations and events in the outside world. The high number of female participants in the sample, in line with the scientific literature, indicates that women have a higher risk of developing depression than men.[29] However, there was no difference between genders in terms of attentional bias in the research findings.

When the diagnostic criteria of major depressive disorder in the DSM-V and the related literature are reviewed, it can be seen that there are findings that individuals develop negative attentional bias as their depression levels increase.[30]

It was previously observed that impairments occur in different information processing associated with depression. One of these deteriorations occurs in memory processes. It is observed that individuals with a diagnosis of depression allocate more attention to negative memories and stimuli, and they have difficulties with bringing back positive memories. When the autobiographical memory processes of individuals with depressive symptoms were examined, it was found that they developed sensitivity to memories with negative content. In studies with individuals having depression diagnosis, the findings indicated that they do not have difficulties with remembering negative memories and do not spend too much time to recall these memories. Ingram also asserted that depression could be an inability to process positive information rather than sensitivity to negative events.[31]

Table 5: Kruskal–Wallis test findings regarding the differentiation of attentional orientation scores according to depression level

The dependent variable	Depression level	n	$\bar{x}$ order	χ^2	P	MW
Attentional orientation	No depression	34	73.50	67,749	<0.001**	1>3
	Mild depression	48	31.49			
	Moderate depression	8	10.56			
	Total	90				

MW: Mann-Whitney *U* test

In a retrospective study conducted by Elgersma *et al*., it was observed that contrary to the literature, and results were obtained in terms of negative attentional bias in wide ranges where depression levels vary. In their study, it was found that patients with different depressive levels did not always cause negative attentional bias in the long term. When considering the result and the findings in similar studies, it can be considered that it is important to conduct in-depth attentional bias studies among individuals having different levels of depressive symptoms to obtain more reliable results.[26]

The findings of this study provide significant results and maybe a guide for further other studies on attentional bias and depression. Despite significant results in terms of understanding the relationship between depression and attentional bias, this study has certain limitations. However, this study is capable of guiding the studies carried out in a large sample, supported by attention performance and attention training techniques. Since the study was carried out with 90 undergraduate and graduate students in three different universities, these findings can be considered limited in terms of generalization of the results for university students. However, it can be considered that this study will contribute to the national literature, which includes limited previous research about the relationship between attentional bias and depression. In addition, measuring attentional bias by using various methods and including participants with different levels of depressive symptoms with a larger sample will be contributive for other studies.

Patient informed consent

Patient informed consent was obtained.

Ethics committee approval

The ethics committee approval has been obtained from Dogus University Committee. (No:E-42435178-050.06.04-36367/Date:14.11.22).

Financial support and sponsorship

No funding was received.

Conflicts of interest

There are no conflicts of interest to declare.

Author contribution subject and rate

- Nazende Ceren Öksüz Özdemir (100%): Design the research, data collection and analyses and wrote the whole manuscript.

References

1. Kolb B, Whishaw I. Fundamentals of Human Neuropsychology. 4th ed. New York: W.H. Freeman and Company; 1996.
2. Eysenck MW, Keane MT. Cognitive Psychology: A Student's Hand Book. Hove, UK: Lawrence Erlbaum Associates Ltd; 2000.
3. Broadbent DE. The effects of noise on behaviour. In: *Perception and Communication*. University of Chicago: Pergamon Press; 1958. p. 81-107.
4. Franken IH, Stam CJ, Hendriks VM, van den Brink W. Neurophysiological evidence for abnormal cognitive processing of drug cues in heroin dependence. Psychopharmacology (Berl) 2003;170:205-12.
5. Johnston R. The determinants of service quality: Satisfiers and dissatisfiers. Int J Serv Ind Manage 1995;6:53-71.
6. Renwick B, Campbell IC, Schmidt U. Attention bias modification: A new approach to the treatment of eating disorders? Int J Eat Disord 2013;46:496-500.
7. Dewitte M, De Houwer J, Koster EH, Buysse A. What's in a name? Attachment-related attentional bias. Emotion 2007;7:535-45.
8. MacLeod C, Mathews A, Tata P. Attentional bias in emotional disorders. J Abnorm Psychol 1986;95:15-20.
9. Mogg K, Bradley BP, Williams R. Attentional bias in anxiety and depression: The role of awareness. Br J Clin Psychol 1995;34:17-36.
10. Koranyi N, Rothermund K. When the grass on the other side of the fence doesn't matter: Reciprocal romantic interest neutralizes attentional bias towards attractive alternatives. J Exp Soc Psychol 2012;48:186-91.
11. American Psychiatric Association. Diagnostic and Statistical Manual of Mental Disorders. DSM-V. 5th ed. Washington: American Psychiatric Association; 2013.
12. Wakefield JC, Lorenzo-Luaces L, Lee JJ. Taking People as they are: Evolutionary Psychopathology, Uncomplicated Depression, and Distinction between Normal and Disordered Sadness. Springer Company; 2017. p. 33-77.
13. Kalınkılıç, E. The Effects of Negative Emotional State on Attention Bias in Smoking and Non-Smoker Young Adult Men. Unpublished Master Thesis. Ankara: Hacettepe University; 2017.
14. Mogg K, Bradley BP. Attentional bias in depressive disorder versus. Generalized Anxiety Disorder. Cogn Ther Res 2005;29:29-45.
15. Bodenschatz C, Scopinceva MM, Rub T, Suslow T. Attentional bias and childhood maltreatment in clinical depression - An eye-tracking The auditory consonant trigram (ACT) test: A norm updating study 2019;112:83-88. doi: 10.1016/j.jpsychires.2019.02.025.
16. Ertan-Kaya Ö, Kademeli M, Salma F, Cangöz-Tavat B, Baran Z. The auditory consonant trigram (ACT) test: A norm updating study for university students. J Appl NeuropsycholAdult 2021;21;1-9. Available from: https://www.tandfonline.com/hapn21. [doi.org/10.1080/23279095.2021.1986509].
17. Taşpınar A, Pakyürek G. The effect of depression level on attention performance in smokers. J Addict 2020;21:34-43.
18. Rantanen M, Hautala J, Loberg O, Nuorva J, Hietanen JK, Nummenmaa L, *et al.* Attentional bias towards interpersonal aggression in depression – An eye movement study. Scand J Psychol 2021;62:639-47.
19. Tran US, Glück TM, Nader IW. Investigating the five facet mindfulness questionnaire (FFMQ): Construction of a short form and evidence of a two-factor higher order structure of mindfulness. J Clin Psychol 2013;69:951-65.
20. Leyman L, De Raedt R, Schacht R, Koster EH. Attentional biases for angry faces in unipolar depression. Psychol Med 2007;37:393-402.
21. Bodenschatz CM, Skopinceva M, Russ T, Suslow T. Attentional bias and childhood maltreatment in clinical depression – An eye-tracking study. J Psychiatr Res 2019;112:83-8.

22. Boyacıoğlu İ, Aktaş, Ç. The relationships between depression and the centrality and phenomenological characteristics of positive and negative autobiographical memories. New Symposium 2020;58:23-30. [doi: 10.5455/nys. 20190914094000].
23. LeMoult J, Joormann J, Kircanski K, Gotlib IH. Attentional bias training in girls at risk for depression. J Child Psychol Psychiatry 2016;57:1326-33.
24. Beevers CG, Clasen PC, Enock PM, Schnyer DM. Attention bias modification for major depressive disorder: Effects on attention bias, resting state connectivity, and symptom change. J Abnorm Psychol 2015;124:463-75.
25. Krings A, Heeren A, Fontaine P, Blairy S. Attentional biases in depression: Relation to disorder severity, rumination, and anhedonia. Compr Psychiatry 2020;100:152173.
26. Elgersma HJ, Koster EH, Vugteveen J, Hoekzema A, Penninx BW, Bockting CL, *et al.* Predictive value of attentional bias for the recurrence of depression: A 4-year prospective study in remitted depressed individuals. Behav Res Ther 2019;114:25-34.
27. Hisli-Sahin NH, Durak A. Brief symptom inventory (BSI): Adaptation for turkish youth a study of the brief symptom inventory in turkish youth. Turk J Psychol 1994;9:44-56.
28. Akdemir A, Örsel SD, Dağ İ, Türkçapar MH, İşcan N, Özbay H. Validity-reliability and clinical use of the Amilton depression rating scale (HDDO). J Psychiatr Psychol Psychopharmacol 1996;4:251-9.
29. MacLeod C, Mathews A, Tata P. Attentional bias in emotional disorders. J Abnorm Psychol 1986;95:15-20.
30. Benoît G, Fortin L, Lemelin S, Laplante L, Thomas J, Everett J. Selective attention in major depression: Clinical retardation and cognitive inhibition. Can J Psychol 1992;46:41-52.
31. Rippere V. Commonsense beliefs about depression and antidepressive behavior: A study of social consensus. Behav Res Ther 1977;15:465-73.

Original Article

Paralyzed Patients-oriented Electroencephalogram Signals Processing Using Convolutional Neural Network Through Python

Vedat Topuz[1], Ayça AK[1], Tülin Boyar[2]

[1]Marmara University, Vocational School of Technical Sciences, Kartal, [2]Marmara University, Faculty of Technology, Department of Computer Engineering, Maltepe, Istanbul, Turkey

Abstract

Aim: Some of the systems that use brain–computer interfaces (BCIs) that translate brain activity patterns into commands for an interactive application make use of samples produced by motor imagery. This study focuses on processing electroencephalogram (EEG) signals using convolutional neural network (CNN). It is aimed to analyze EEG signals using Python, convert data to spectrogram, and classify them with CNN in this article. **Materials and Methods:** EEG data used were sampled at a sampling frequency of 128 Hz, in the range of 0.5–50 Hz. The EEG file is processed using Python programming language. Spectrogram images of the channels were obtained with the Python YASA library. **Results:** The success of the CNN model applied to dataset was found to be 89.58%. **Conclusion:** EEG signals make it possible to detect diseases using various machine learning methods. Deep learning-based CNN algorithms can also be used for this purpose.

Keywords: *Electroencephalogram, convolutional neural network, spectrogram images*

Introduction

Analysis of biomedical signals has become one of the hottest topics with advances in technology and machine learning. Researchers are working to understand and classify human biosignals to more accurately diagnose diseases or develop assistive technologies for people with disabilities.[1] Electroencephalogram (EEG) brain signals are one of the most studied topics for developing noninvasive approaches to detect neurological abnormalities and brain–computer interface (BCI) technologies.[2]

Today, motor imagery (MI) EEG-based BCI is studied by many researchers due to its effectiveness in both nonmedical and medical applications. MI is accomplished by imagining executing a particular command without actually doing it. MI tasks commonly used in research are movements related to the left hand, right hand, left foot, right foot, both feet, elbows, fists, and fingers. MI-based BCI applications include clarifying the EEG signals and defining the responses to these signals in real time.[3] It has laid the groundwork for interesting studies such as the processing of EEG signals, robot movements with thought, and detection of various diseases according to brain activity.

The data set, which is frequently used in studies for the diagnosis of diseases related to brain activity, was taken from the University of Bonn database.[4] Türk and Özerdem (2017) aimed to classify the features extracted from EEG signals using the One-Dimensional Median Local Binary Pattern method with the k-nearest neighbor (k-NN) algorithm.[5] The data used in the study were taken from Bonn data set.[4] In the study, the classification performance was found to be 100% for A-E datasets, 99.00% for A-D datasets, 98.00% for D-E datasets, 99.50% for CD-E datasets, and 96.00% for A-D-E datasets. When the effect of the one dimension median local binary pattern method on classification in EEG datasets is compared with other studies, it was seen that the proposed approach gave successful results.[5] Çevik worked on an application that allows vehicle control by detecting the physical and mental states of the operators (such as fatigue, sleepiness, and inattention) through EEG signals for vehicle use. Fast Fourier transform (FFT) and power spectral density (PSD) signal processing techniques are used for feature extraction from

How to cite this article: Topuz V, Ayça AK, Boyar T. Paralyzed patients-oriented electroencephalogram signals processing using convolutional neural network through python. J Neurobehav Sci 2022;9:90-5.

Ethics committee approval: There is no need for ethics committee approval.

Received : 04-12-2022
Revised : 06-12-2022
Accepted : 11-12-2022
Published : 29-12-2022

Orcid
Vedat Topuz: {ORCID: 0000-0001-7461-1849}
Ayça AK: {ORCID: 0000-0002-3429-4962}
Tülin Boyar: {ORCID: 0000-0002-5797-1284}

Address for correspondence:
Prof. Vedat Topuz, Vocational School of Technical Sciences, Marmara University Mehmet Genç Kulliyesi, Dragos, Kartal, Istanbul 34865, Turkey.
E-mail: vtopuz@marmara.edu.tr

Access this article online

Website: www.jnbsjournal.com

DOI: 10.4103/jnbs.jnbs_33_22

Quick Response Code:

signals.[6] Akben conducted a comprehensive research on the characteristics and diagnosis of migraine disease using EEG signals in his study (2012). The data obtained from the KSU Faculty of Medicine used in the study belong to 30 migraine patients and 30 healthy controls. The data were first analyzed with the Fourier transform on the frequency axis. The results were analyzed with the help of classification techniques and clustering techniques. As a result, some characteristic data about migraine disease have been obtained and different suggestions have been made for the automatic diagnosis of the disease.[7] Coşkun and Istanbullu analyzed EEG data from a patient under anesthesia with different methods such as band-pass filter, FFT, wavelet transform, and PSD.[8]

Olivas-Paddal and Chacon-Murguia proposed two methods for multimotor image classification. Both methods use features obtained with a variant of the discriminatory Filter Bank Common Spatial Model. One method uses convolutional neural network (CNN) classification, whereas the second method uses a modular network of four expert CNNs.[9] Hernández-Del-Toro *et al*. present five feature extraction methods based on fractal dimension, wavelet decomposition, frequency energies, empirical mode decomposition, and chaos theory properties to solve the task of detecting MI segments.[10]

In this article, the classification of EEG signals has been carried out by converting them to spectrogram images. It is explained how these operations are performed with Python. A CNN is designed for the classification process. The rest of the article is organized in the following sections. The material and method are described in Section 2. The results obtained are presented in Section 3. In Section 4, a general evaluation of the study is made.

Materials and Methods

There is no need for ethics committee approval.

Electroencephalography (EEG) is a method that provides electrical induction of brain activity. EEG recording is performed by placing conductive wires on the skull with the help of a special gel. The electrical potential changes between these placed electrons are recorded on the computer by means of an analog–digital converter. This recording can be used in studies such as the detection of diseases using various transformations.

Brain activity is related to the frequencies of EEG signals. In clinical studies, the frequencies of EEG signals in the range of 0.5–30 Hz are examined. Frequencies above 30 Hz are known as gamma signals. Because their amplitudes are so low, they are not significant and are rarely used. Table 1 shows the frequency bands and frequency ranges to which EEG signals may belong.

Delta waves are seen in infants and severe organic brain diseases. Theta waves particularly arise in children. In adults, they also occur in situations of emotional tension and frustration. Alpha waves are seen in awake, normal, and calm people. They

Table 1: Electroencephalogram signal bands and frequencies

EEG frequency band	Frequency range (Hz)	Amplitude (μV)
Delta (δ)	0.5-4	20-400
Theta (θ)	48	5-100
Alfa (α)	8-13	2-10
Beta (β)	13-30	1-5
Gama (γ)	30+	1+

+: Plus, EEG: Electroencephalogram

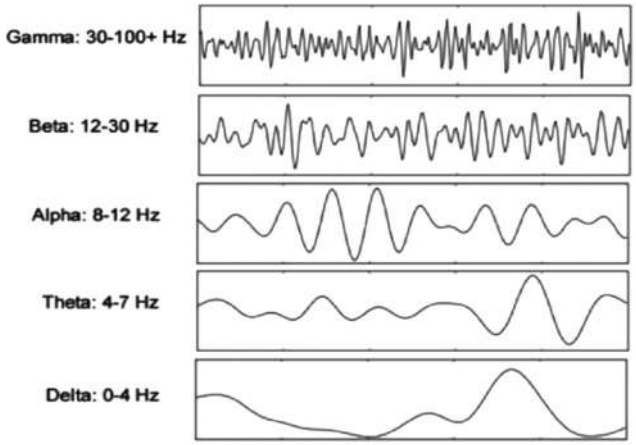

Figure 1: EEG bands.[1] EEG: Electroencephalogram

disappear into the dormant state. If the awake person directs his attention to something special, higher frequency but lower amplitude EEG signals (Beta waves) occur instead of α waves. Beta waves occur in strong activation of the central nervous system or states of tension. They disappear with increased mental activity and are replaced by low-amplitude asynchronous signs. Gamma waves are used a lot in clinical practice when their amplitudes are very small and meaningless. Waves in different frequency ranges of EEG signals are shown in Figure 1.[11]

Data reading and display

Ethics committee report is not required since it has not been tested on paralyzed patients yet. The data used were sampled at a sampling frequency of 128 Hz, in the range of 0.5–50 Hz, belonging to 29 channels. The EEG log file is opened with the Python programming language MNE library [Figure 2].

```
#read files
file = "a.edf"
raw = mne.io.read_raw_edf(file,preload=True)
print(raw)
print(raw.info)
raw.crop(tmax=60)
eeg_and_eog = raw.copy().pick_types(meg=False, eeg=True, eog=True)
print(len(raw.ch_names), '→', len(eeg_and_eog.ch_names))
print(raw.ch_names[-3:])
channel_renaming_dict = {name: name.replace(' ', '_') for name in
raw.ch_names}
raw.rename_channels(channel_renaming_dict)
print(raw.ch_names[-3:])
```

Channel signals can be accessed on the ".edf" file with the Python MNE library. Image of a specific channel or more

than one channel can be taken. The graph in Figure 3 is plotted over Python using the following code; it shows the synchronous signal of all channels.

```
sampling_freq = raw.info['sfreq']
start_stop_seconds = np.array([11, 13])
start_sample, stop_sample = (start_stop_seconds *
sampling_freq).astype(int)
channel_index = 0
raw_selection = raw[channel_index, start_sample:stop_sample]
print(raw_selection)
x = raw_selection[1]
y = raw_selection[0].T
#plot all channels
plt.plot(x,y)
```

The signals of the EEG-A1 and EOG-2 channels are shown in Figure 4 as plotted over Python using the following code.

```
<RawEDF | a.edf, 29 x 64768 (506.0 s), ~14.4 MB, data loaded>
<Info | 7 non-empty values
 bads: []
 ch_names: EEG A1, EEG Fp1, EEG A2, EEG F7, EEG F8, EEG T3, EEG T4, EEG T5, ...
 chs: 29 EEG
 custom_ref_applied: False
 highpass: 0.5 Hz
 lowpass: 50.0 Hz
 meas_date: 2021-10-28 10:49:28 UTC
 nchan: 29
 projs: []
 sfreq: 128.0 Hz
```

Figure 2: Data set information

```
channel_names = ['EEG A1', 'EOG-2']
two_meg_chans = raw[channel_names, start_sample:stop_sample]
y_offset = np.array([5e-11, 0])  # just enough to separate the channel
traces
x = two_meg_chans[1]
y = two_meg_chans[0].T + y_offset
lines = plt.plot(x, y)
#plot two selection
plt.legend(lines, channel_names)
print(raw.info)
#plot one channels fmax=50
raw.plot_psd(fmax=50)
raw.plot(duration=5, n_channels=30)
```

Specific events on the data can be detected with the "events" subcommand. In some data, events are captured from STIM channels.

```
mne.find_events(raw, stim_channel='STI 014')
```

Some EEG/MEG systems create files in which events are stored in a separate data stream rather than pulses on one or more STIM channels. For example, the EEGLAB format stores events as a collection of arrays in the.set file. When reading these files, MNE-Python automatically converts the stored events into an annotations object and stores it as an annotation attribute of the raw object. The underlying data in an annotations object can be accessed through its three attributes: start, duration, and description.

In the EEG data used as an example, the events are stored in a separate data series. To read event information:

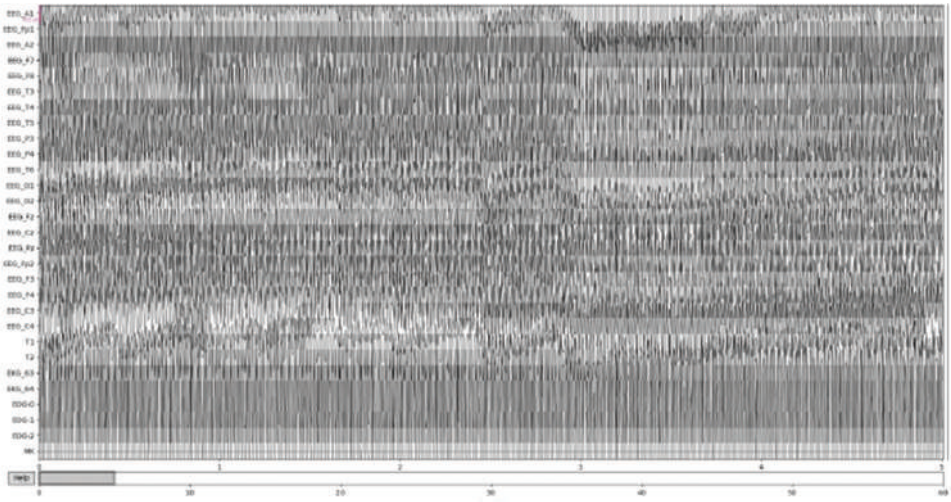

Figure 3: Signals of all channels

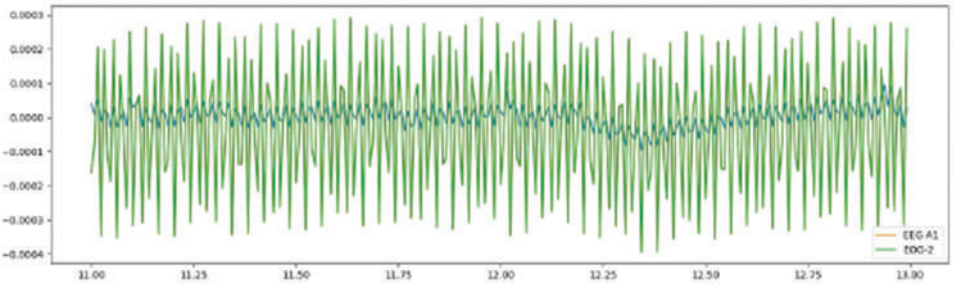

Figure 4: EEG A1 and EOG 2 signals. EEG: Electroencephalogram

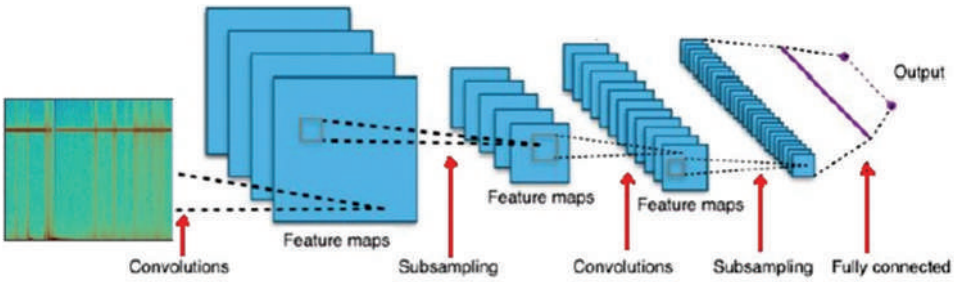

Figure 5: Convolutional neural network

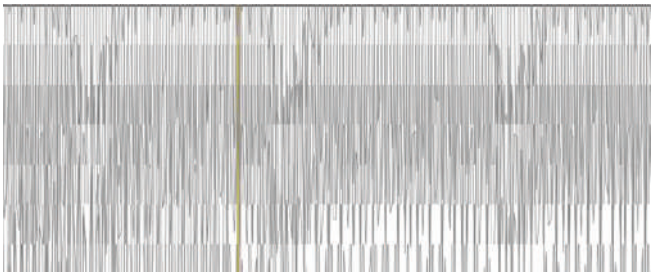

Figure 6: Image of an event on a signal

```
sample_data_raw_file = 'a.edf'
raw = mne.io.read_raw_edf(sample_data_raw_file)
#detect events from annotation
events_from_annot, event_dict = mne.events_from_annotations(raw)

events=mne.events_from_annotations(raw,event_id="auto")
print(events[0])
print(events[1])
```

Convolutional neural network

Recently, studies have been carried out on the use of CNN algorithms, which are a deep learning model on EEG signals[12-14] CNN is a feedforward neural network, which is a type of multilayer perceptron.[15] CNN consists of convolutional layer, pool layer, and fully connected layers. Figure 5 shows the representation of a CNN structure. When the image is given as input to a network, it feeds the system through interconnected polyconvolutions and finally produces an output.[16]

In the convolution layer, there are filters to extract features from the image given as input. Images are saved in matrix format and feature matrix called kernel is used to extract features. Convolution is a mathematical function that expresses how one shape changes by another:

$$|f * g| \equiv \int_0^\tau f(\tau)g(t-\tau)d\tau \quad (1)$$

Convolution operation is performed by shifting the convolution filter on the image matrix. Conflicting numbers are multiplied and transferred to the feature map matrix. With this operation, the size of our input image is reduced. However, this also causes image distortions. To prevent data loss, the same padding method, which is performed by adding a frame of zero values around the input image, is used. Since the feature map holds a certain part of the image, a large number of feature maps are needed. After the convolution process, the ReLu function is applied to reset the negative values.[17]

Results

Here in the "events" array received in the annotation object, events [0]→ event descriptions, events [1]→ event start time, and event identification number (ID) information are kept. To see the events on the signal, the signals received from all channels were plotted and colored during the recording and the event was detected on the signal. The image of the left leg raising and lowering event on the signal are shown in Figure 6. The ID-time graph of the events is shown in Figure 7.

```
sample_data_raw_file = 'a.edf'
raw = mne.io.read_raw_edf(sample_data_raw_file)
raw_temp=raw.copy()
#Dropped last 8 channels
raw_temp.drop_channels(['T1', 'T2', 'EKG 63', 'EKG 64', 'EOG-0', 'EOG-
1', 'EOG-2', 'MK'])
#selection time
raw_selection = raw_temp.copy().crop(tmin=262, tmax=263)
events=mne.events_from_annotations(raw_selection)
events_from_annot, event_dict =
mne.events_from_annotations(raw_selection)
raw_selection.plot(start=0,duration=4)
```

Since the first 21 channels contain information about the EEG data, the other nine channels' information has been removed. Annotation objects detected in the data were obtained with their ids as "events_dict."

Drawing channel spectrograms with YASA Library

Spectrogram images of the channels can be obtained With the Python YASA library. The code block below is for obtaining the spectrogram image of channel 20 [Figure 8].

```
npz = np.load('my_data.npy')
arr=np.array(npz)
arr_trans=arr.transpose()
print(arr_trans)
# fig = yasa.plot_spectrogram(data, sf)
print(len(arr_trans))
data = arr_trans[0,:]
print(data)
#Draw Figure For Example Channel
sf = 100
data = npz[20]
 #draw 1 channel
fig = yasa.plot_spectrogram(data, sf)
print("Figure"+str(20)+":"+str(raw.ch_names[19]))
```

In addition, spectrogram image can be obtained for each event with "plt.specgram" (spectrogram image for *ID = 1* event) [Figure 9].

Obtaining epoch objects with MNE library

The "epochs" object in the library was used to analyze the events in detail to extract the events in the data. After converting the events into epoch objects, operations such as reading the signal values of the events and saving them in the ".csv."

Application of CNN algorithm to electroencephalogram data

First, Python's deep learning libraries Keras and TensorFlow are included for data processing with CNN. In the ".csv" file, the values obtained from 21 channels are input and events are output. The events are numbered from 1 to 6, respectively, by converting them to category type. An example image with a sample signal for each category is presented in Figure 10.

First, 80% of the data set is reserved as training data and 20% as test data:

```
X_train, X_test, Y_train, Y_test = train_test_split(X, Y,
test_size=0.20, random_state=1)test_size=0.20, random_state=1
```

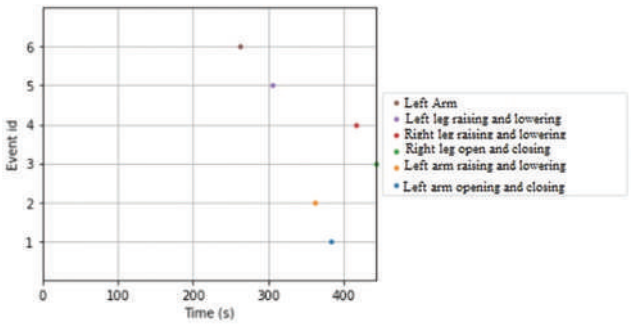

Figure 7: Occurrence time of events

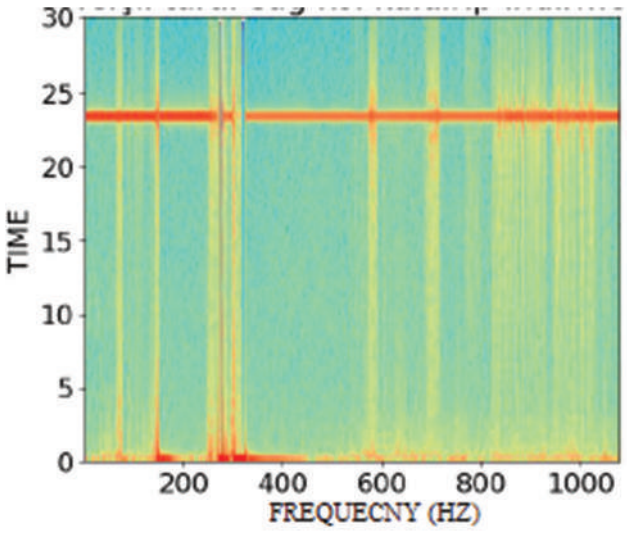

Figure 9: Spectrogram image for ID 1

The CNN structure generated using the following code is shown below.

```
model = Sequential()
model.add(Conv1D(filters=2048, kernel_size=3, activation='relu',
input_shape=(21,1)))
model.add(Dropout(0.5))
model.add(Conv1D(filters=1024, kernel_size=3, activation='relu'))
model.add(Dropout(0.5))
model.add(Conv1D(filters=512, kernel_size=3, activation='relu'))
model.add(Dropout(0.5))
model.add(Conv1D(filters=256, kernel_size=3, activation='relu'))
model.add(Dropout(0.3))
model.add(Conv1D(filters=128, kernel_size=3, activation='relu'))
model.add(Dropout(0.3))
model.add(Conv1D(filters=128, kernel_size=3, activation='relu'))
model.add(Dropout(0.3))
model.add(Conv1D(filters=64, kernel_size=3, activation='relu'))
model.add(Dropout(0.3))
model.add(Conv1D(filters=32, kernel_size=3, activation='relu'))
model.add(Dropout(0.3))
model.add(MaxPooling1D(pool_size=2))
model.add(Flatten())
model.add(Dense(6, activation='softmax'))
model.summary()
```

CNN was trained with the training data set and results were obtained with the test data set. The accuracy value was 89.58%. The data on the success of our model are shown in Figure 11.

Conclusion

In this article, it is aimed to examine EEG signals with Python. For this purpose, first of all, the EEG signal and then the spectrogram of this signal were visualized with Python. A CNN structure was designed to classify the obtained spectrogram image. As a result of the trials with the test data, it was determined which movement the data belonged to with an accuracy of 89.5%. This study can be

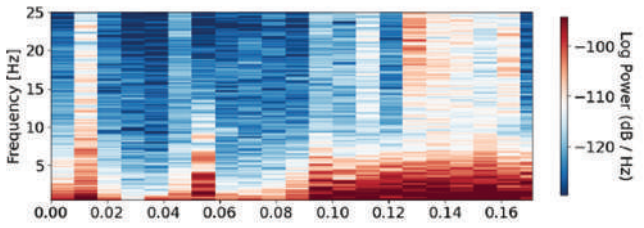

Figure 8: Spectrogram image

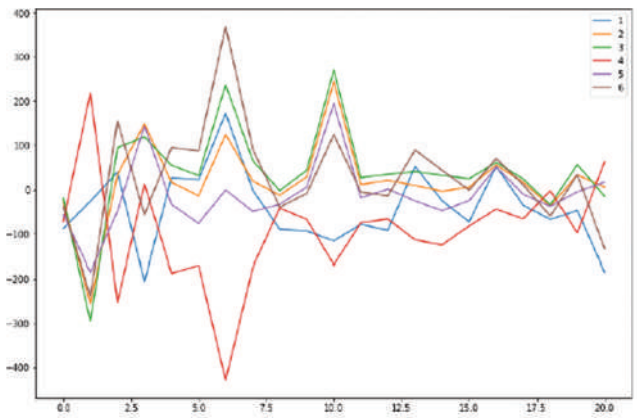

Figure 10: Signals

	precision	recall	f1-score	support
0	1.00	0.83	0.91	454
1	0.57	0.52	0.55	477
2	0.64	0.42	0.51	472
3	0.93	0.76	0.84	422
4	0.80	0.78	0.79	475
micro avg	0.79	0.66	0.72	2300
macro avg	0.79	0.66	0.72	2300
weighted avg	0.78	0.66	0.71	2300
samples avg	0.66	0.66	0.66	2300

accuracy: 89.58%

Figure 11: Accuracy

improved by studies such as device control with data from paralyzed individuals.

Patient informed consent

There is no need for patient informed consent.

Ethics committee approval

There is no need for ethics committee approval.

Conflicts of interest

There are no conflicts of interest to declare.

Financial support and sponsorship

No funding was received.

Author contribution subject and rate

- Vedat TOPUZ (35%): Design the research, Contributed with comments on manuscript organization and write-up.
- Ayça AK (30%): Contribute the research, Analyses and wrote the whole manuscript.
- Tülin BOYAR (35%): Realise the research. Implementing the software.

References

1. Cinar E, Sahin F. New classification techniques for electroencephalogram (EEG) signals and a real-time EEG control of a robot. Neural Comput Appl 2013;22:29-39.
2. Lotte F, Congedo M, Lécuyer A, Lamarche F, Arnaldi B. A review of classification algorithms for EEG-based brain-computer interfaces. J Neural Eng 2007;4:R1-13.
3. Al-Saegh A, Dawwd SA, Abdul-Jabbar JM. Deep learning for motor imagery EEG-based classification: A review. Biomed Signal Process Control 2021;63:102172.
4. Available from: https://www.ukbonn.de/epileptology/donate-to-the-verein-zur-foerderung-der-epilepsieforschung-ev/. [Last accessed on 2022 Nov 28].
5. Türk Ö, Özerdem MS. Epileptik EEG sinyallerinin sınıflandırılması için bir boyutlu medyan yerel ikili örüntü temelli öznitelik çıkarımı. Gazi Üniversitesi Fen Bilimleri Dergisi Part (c) 2017;5:97-107.
6. Çevik, Ç. Vehicle management with attention value obtained using brain signals. J Smart Syst Res (JOINSSR) 2020;1:30-8.
7. AkbenSB. İşaret Işleme Teknikleri Kullanarak EEG Işaretlerinden Migren Hastaliğinin Karakteristiklerinin Belirlenmesi, Thesis, Kahramanmaraş Sütçü İmam Üniversitei Fen Bilimleri Enstitüsü; 2012.
8. Coşkun M, İstanbullu A. Analysis of EEG Signals with FFT and Wavelet Transform, Akademik Bilişim'12- XIV. Academic Informatics Conference Proceedings, Uşak University; 2012.
9. Olivas-Padilla BE, Chacon-Murguia MI. Classification of multiple motor imagery using deep convolutional neural networks and spatial filters. Appl Soft Comput J. 2019;75:461-72.
10. Hernández-Del-Toro T, ReyesGarcia CA, Villasenor-Pineda L. Toward asynchronous EEG-based BCI: Detecting imagined words segments in continuous EEG signals. Biomed Signal Process Control 2021;65:102351.
11. Nacy S, Kbah S. Controlling a servo motor using EEG signals from the primary motor cortex. Am J Biomed Eng 2016;6:139-46.
12. Mao WL, Fathurrahman HI, Lee Y, Chang TW. EEG dataset classification using CNN method. J Phys 2019;1456. [doi: 10.1088/1742-6596/1456/1/012017].
13. Ma M, Cheng Y, Wei X, Chen Z, Zhou Y. Research on Epileptic EEG Recognition Based on Improved Residual Networks of 1-D CNN and indRNN. International Conference on Health Big Data and Artificial Intelligence; 2021.
14. Zhou M, Tian C, Cao R, Wang B, Niu Y, Hu T, *et al*. Epileptic seizure detection based on EEG signals and CNN. Neuroinformatics 2018;12:95.
15. Şeker, A., Diri, B. and Balik, H. H. A review of deep learning methods and applications. Gazi Univ J Eng Sci 2017;3:47-64. [doi: 10.3389/fninf.2018.00095].
16. Available from: https://www.datacamp.com/community/tutorials/convolutional-neural-networks-python. [Last accessed on 2022 Nov 28].
17. Available from: https://mgminsights.com/2021/09/19/convolutional-neural-network-cnn-nedir/. [Last accessed on 2022 Nov 28].

Original Article

Design of Magnetoencephalography-based Brain–machine Interface Control Methodology through Time-varying Cortical Neural Connectivity and Extreme Learning Machine

Abstract

Introduction: Human-machine interfaces (HMIs) can improve the quality of life for physically disabled users. This study proposes a noninvasive BMI design methodology to control a robot arm using MEG signals acquired during the user's imagined wrist movements in four directions. **Methods:** The BMI uses the partial directed coherence measure and a time-varying multivariate adaptive autoregressive model to extract task-dependent features for mental task discrimination. An extreme learning machine is used to generate a model with the extracted features, which is used to control the robot arm for rehabilitation or assistance tasks for motor-impaired individuals. **Results:** The classification results show that the proposed BMI methodology is a feasible solution with good performance and fast learning speed. **Discussion:** The proposed BMI methodology is a promising solution for rehabilitation or assistance systems for motor-impaired individuals. The BMI provides satisfactory classification performance at a fast learning speed.

Keywords: *Brain–machine interface, extreme learning machine, functional connectivity, magnetoencephalography*

Caglar Uyulan

Department of Mechanical Engineering, Faculty of Engineering and Architecture, İzmir Katip Celebi University, İzmir, Turkey

Introduction

Brain–machine interfaces (BMIs) are built as communication devices that encode brain activity to a machine command signal, not involving muscles. The utilization of BMIs is quite helpful for users having diseases or traumatic injuries which cause muscle control degradation or motor disabilities (termed as a locked-in syndrome). The locked-in syndromes may comprise a wide spectrum of diseases and traumata, i.e., amyotrophic lateral sclerosis, cerebral palsy, muscular dystrophy, multiple sclerosis, brainstem stroke, and brain or spinal cord injury.

Practical applications of brain–computer interfaces (BCIs) cover electrophysiological signals, such as electroencephalography (EEG), electrocorticography, and MEG. BCIs generally control a robotic end system via these aforementioned signals recorded from the synchronized activity of neuron groups inside the brain of subjects. The subjects can be people having different ages, gender, and physical characteristics. The aim here is to establish a user-independent, generic model of the BMI and to search for robust-adaptive algorithms that minimize the variance of classification errors concerning the various kinds of users. The combination of "feature extraction/dimension reduction/feature selection/classification" algorithms with the best classification performance and the least possible error variance concerning users becomes the main model. As a result of this main model obtained, i.e., the robot trajectory control can be realized. The strong hypothesis (model) that is generated, is expected to guarantee the mental task classification of random users by limiting their errors to a lower band. As a result of this research, the BMI can be brought to a level that competes with commercial applications. The design procedure is divided into three basic modules: data acquisition, signal processing, and machine control. The majority of brain waves along the scalp are collected, and the wave information is transferred to a central processing unit (CPU) for processing in

How to cite this article: Uyulan C. Design of magnetoencephalography-based brain–machine interface control methodology through time-varying cortical neural connectivity and extreme learning machine. J Neurobehav Sci 2022;9:96-106.

Ethics committee approval: There is no need for ethics committee approval

Received : 07-12-2022
Accepted : 11-12-2022
Published : 29-12-2022

Orcid
Caglar Uyulan: {ORCID: 0000-0002-6423-6720}

Address for correspondence:
Dr. Caglar Uyulan, Department of Mechanical Engineering, Faculty of Engineering and Architecture, İzmir Katip Celebi University, İzmir, Turkey.
E-mail: caglaruyulan1@gmail.com

Access this article online

Website: www.jnbsjournal.com

DOI: 10.4103/jnbs.jnbs_35_22

Quick Response Code:

the data acquisition process. The CPU filters the signals and runs algorithms that extract features to control the machine. MEG can decrease training time while increasing the robustness of a BMI. As compared to the EEG, MEG has a larger number of sensors. Therefore, the spatial resolution is more. The detection of the frequency information can be above 40 Hz, which is not capable in EEG recordings.[1,2]

BMI architecture to be designed: (1) should adapt to nonstationary brain dynamics, (2) should generate neural signals from general brain states independently of the users, (3) should have a generalizable structure that will allow an easy transition to control applications, and (4) should demonstrate high classification performance.[3-6]

EEG-based BCIs suffer the problem that the recorded signal is nonstationary, that is, the data are subject to covariate shift. The nonstationarity can occur from the transition of the training model without feedback to online use with feedback, the shift of sensors to different brain regions due to head movements in MEG, or variations in mental status over time. These nonstationary cases are valid for a classifier trained on training data showing this mismatch.[7,8]

Since the MEG is a nonstationary signal, many feature extraction methods that originated from time-domain, frequency-domain, and time-frequency domain analysis, are utilized in the literature.[9-12] Time-domain features are extracted directly from the signal and focus on the (averaged) time course. Frequency-domain features highlight the signal power in frequency band components. Time-frequency domain features analyze how the power spectrum changes with respect to time. The short-time Fourier transform and the wavelet transform are the most applicable.[13-16]

Spatial filtering, which extracts signals from multiple sensors to look at the activity localized in a particular brain region, is also applied. Some of the common spatial filtering methods can be listed as: *bipolar montage*, where bipolar channels are evaluated by subtracting the signals from two collocated electrodes;[17] *common average reference*, which subtracts the average value of the full electrode montage from that of the specific channel;[18] *Laplacian method,* which evaluates for each electrode location the second derivative of the instantaneous spatial voltage distribution by combining the value at that location with the values of a set of surrounding electrodes;[19] and *common spatial patterns*, which analyzes multichannel data based on savings from two tasks. The filters are utilized to optimize the variance for one task and minimize it for the other tasks.[20] Other techniques have also been utilized in electrophysiological feature extraction, such as the Kalman filter, fractal dimensions, and entropy.[21-23] The AAR algorithm based on the Kalman filtering approach has also been applied to analyze the electrophysiological signals. The parametric model has an adaptive closed-loop controller with a recursive Bayesian estimator and a linear-square regulator. It estimates states and system parameters from different mental tasks and feeds them back to the optimal controller. The performance of BMIs is enhanced by closed-loop solver adaptation or multiplicative recurrent artificial neural network (ANN) solver coupled with KF. Thanks to this solver, the learned training datasets become more robust and provide a wide variety of neural-kinematic mapping learning.[24-26]

Coming to the classification stage, the use of ANNs is quite common. However, the learning rates of feedforward ANNs, including deep learning applications, are quite low. Among the main reasons for this are the use of slow gradient-based learning algorithms in the training of ANNs and the iterative updating of all parameters of the networks in this way at each stage. ELMs have succeeded in solving this problem by proving that hidden nodes do not necessitate learning and are recursively set. ELM consists of generalized single or several hidden layer feedforward networks. ELMs give importance to feature representations in hidden layers compared to support vector machines (SVMs). These models can demonstrate good generalization performance and learn extremely faster than backpropagation networks. Random input layer weights add to the generalization capabilities of a linear output layer solution as it has nearly orthogonal (weakly correlated) hidden layer properties. If the weight range is constrained, the orthogonal inputs yield a larger solution space volume with these constrained weights. Thanks to the small-weight norms, the system is more stable and robust to noise. The random hidden layer generates weakly correlated hidden layer features, proposing a solution with a low norm and strong generalization performance. Various types of ELM have been proposed in the literature.[27-29]

To learn effectively from various data types, ELMs need to be modified to suit the problem. When new samples are added to the dataset and grown, the ELM is retrained, but retraining the network is inefficient because the proportion of new incoming data is small. Therefore, Matias *et al.*[30] proposed an online sequential ELM (OS-ELM). The basic idea behind OS-ELM is to avoid retraining on previous examples using a sequential method. OS-ELM reconstructs settings using new instances sequentially after startup. Huang *et al.*[31] developed an incremental ELM (I-ELM). When a new hidden node is introduced, I-ELM randomly adds nodes to the hidden layer one by one, freezing the output weights of the existing hidden nodes. I-ELM is effective for single-layer feedforward networks (SLFNs) with piecewise continuous activation functions. Rong *et al.*[32] proposed a pruned ELM (P-ELM) algorithm as a systematic and automated strategy for building ELM networks. Using a small number of hidden nodes can

cause under/overfitting problems in model classification. Compared to traditional ELM, simulation results showed that P-ELM results in compact network classifiers that produce fast responses and strong prediction accuracy on unseen data. Feng *et al.*[33] proposed an error minimization-based method (EM-ELM) that determines the number of hidden nodes in generalized SLFNs by growing hidden nodes one by one or group by group. As the networks grow, the output weights are gradually changed, significantly reducing the computational burden. The simulation results in sigmoid-type hidden nodes showed that this method can greatly decrease the computational cost of ELM. Nodes are randomly added to the network until they reach a certain error value of ε. A new learning algorithm called an evolutionary ELM (E-ELM) has been developed to optimize input weights and latent biases and determine output weights. Output weights are determined analytically using the MP generalized inverse.[34] The stability and generalization performance of the ELM was investigated. This system consists of two stages. In the first step, a forward iterative algorithm is applied to select hidden nodes from randomly generated candidates at each step and then hidden nodes are added until the stopping criterion is matched. In the second stage, unimportant nodes are removed.[35,36] A kernel-based ELM (KELM) inspired by SVM has been developed and the main kernel function used in ELMs is the radial basis function. KELMs are used to design deep ELMs (DELMs).[37] DELMs utilize KELM as an output layer.[38] Voting-based ELM (V-ELM) has been proposed to improve performance on classification tasks. In V-ELM, not just one network is trained, but also many are trained and then the fittest is chosen according to the majority voting method.[39]

In this study, a signal processing methodology was developed for the subjects who control the movement of a robotic arm using four motor imagery signals related to the following wrist movement states, respectively: right, forward, left, and backward. Section 2 gives a background on the MEG acquisition system and the robot arm, followed by a discussion on the classification and control strategy implemented in this study. In Section 3, the analysis results were presented. Section 4 includes the discussion and conclusive summary part.

Materials and Methods

There is no need for ethics committee approval.

MEG data acquisition and preprocessing

The data set was provided by the Brain Machine Interfacing Initiative, Albert-Ludwigs-University Freiburg, the Bernstein Center for Computational Neuroscience Freiburg, and the Institute of Medical Psychology and Behavioral Neurobiology, the University of Tübingen collected for the BCI Competition IV (https://www.bbci.de/competition/iv/). The data set comprises directionally modulated low-frequency MEG activity that was acquired from two healthy, right-handed subjects. They performed wrist movements in four various directions, i.e., we have four different classes. The task was to move a joystick from a center position toward one of four targets located radially at 90° intervals (four-class center-out paradigm) utilizing exclusively the right hand and wrist.

The MEG device has 10 channels and 625 Hz. sampling rate. The data were band-pass filtered (0.5 to 100 Hz., Butterworth, 3rd order) and resampled at 400 Hz. The data comprise signals from ten MEG channels which were positioned above the motor areas given in Figure 1.

The details about the data acquisition and signal processing processes can be accessed at https://www.bbci.de/competition/iv/. Data were collected from two separate subjects including training sessions during 40 s/trials for each mental task, and testing sessions during 73 trials by executing random tasks. The test data will be used as external validation for assessing the performance of the proposed classifier.

The training data were merged as the size of the matrix for each mental task-based class is 40 (number of trials)×800 (number of sampling data)×10 (number of channels). The train data matrix was reshaped into a two-dimensional form as 32000 (number obtained from multiplication of trials with the sampling data)×(number of channels). The total size of the training data is 128000 × 10.

The testing data including the random sequence of mental tasks were merged as the size of the matrix is 73 (number of trials)×800 (number of sampling data)×10 (number of channels). The test data matrix was reshaped into a two-dimensional form as 58400 (number obtained from multiplication of trials with the sampling data)×10 (number of channels).

Feature extraction

The feature extraction process includes the transformation of the preprocessed signal into a feature matrix by attenuating noise and focusing on important data. The AR_{FIT} package is utilized to find an optimum model order for the time-varying multivariate autoregressive (MVAR) model. The time-invariant parameter and the order of the model can be estimated using AR_{FIT}-package. "Schwarz's Bayesian Criterion" is applied for the order estimation and then the model order is fixed for further analysis. Time-varying partial directed coherences (PDCs) are evaluated through the time-varying MVAR model matched with the signal using an AAR algorithm, which uses linear Kalman filtering for parameter estimation. A surrogate

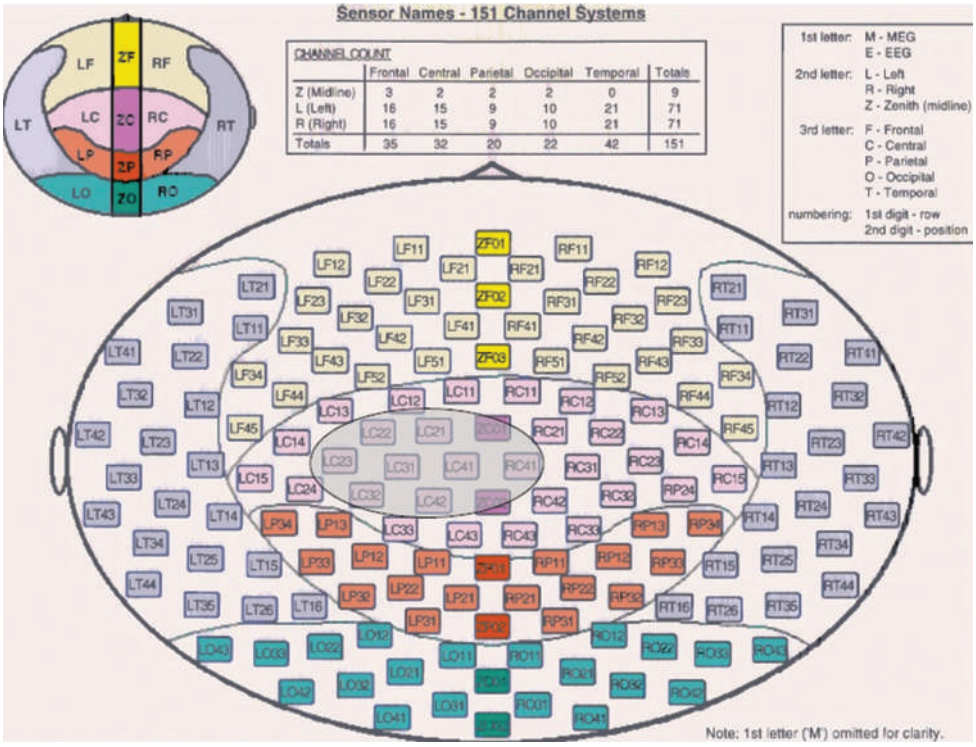

Figure 1: The MEG channel positions. 'LC21', 'LC22', 'LC23', 'LC31', 'LC32', 'LC41', 'LC42', 'RC41', 'ZC01', 'ZC02' [https://www.bbci.de/competition/iv/]

data method having 50 realizations is performed to choose the most essential quantities of the measure at a 99% confidence level. Surrogates are constructed by randomizing all samples of the signal to remove the causal relations among them.[40,41] The algorithm embeds the linear Kalman filtering to update the MVAR parameters for each time sample.

A *d*-dimensional time-varying MVAR process is given in Eq. 1.

$$y_k = \sum_{r=1}^{p} A_k^{(r)} y_{k-r} + w_k \tag{1}$$

where p is the model order, $w_k \in R^d$ is a zero-mean white process noise vector, and $A_k^{(r)} \in R^{d\times d}$ is the matrix of autoregressive coefficients at each lag r and time point $k=p+1,\ldots,N$.

A form of state space equations is built from the MVAR equations by re-organizing all matrix parameters into a state vector of the dynamical system and focusing the nonstationary signal as the measurement is given in Eq. 2.[42,43]

$$\begin{aligned} x_k &= F_{k-1} x_{k-1} + K_k e_k \\ y_k &= H_k x_k + v_k \end{aligned} \tag{2}$$

where x_k is the parameter vector (state vector), k_k is the Kalman gain, H_k is the measurement matrix (observation matrix), e_k is the one-step prediction error, and y_k is the estimated vector.

x_k and H_k are stated in Eq. 3.

$$x_k = \begin{bmatrix} x_{11}(1,k) \\ . \\ . \\ . \\ x_{1m}(p,k) \\ . \\ . \\ . \\ x_{m1}(1,k) \\ . \\ . \\ . \\ x_{mm}(p,k) \end{bmatrix}, \quad H_k = \begin{bmatrix} y^T(k-1) & . & . & . & 0 \\ . & . & . & . & . \\ . & . & . & . & . \\ . & . & . & . & . \\ 0 & . & . & . & y^T(k-1) \end{bmatrix} \tag{3}$$

where $y^T(k-1)=[y^T(k-1)\ldots y^T(k-p))]$. The elements of the state vector are estimated via the Kalman filtering approach. The process and observation noise covariance matrices $(w(k),v(k))$are updated using a specific method given in Eq. 4.[44]

$$\begin{aligned} v(k) &= (1-\zeta)\times v(k-1) + \zeta \times e(k) \\ w(k) &= \left(I \times \zeta \times tr(z(k))\right) \Big/ p \end{aligned} \tag{4}$$

where ζ is the update coefficient, $z(k)$ is the a-posteriori correlation matrix. I is the identity matrix, and × implies the matrix product operator.

The update coefficient determines the time resolution and the smoothing of the AR estimates. The $A_k^{(r)}$ matrices given in Eq. 1 are in the following form given in Eq. 5.

$$A_k^{(r)} = \begin{bmatrix} a_{11}(r,k) & . & . & . & a_{1N}(r,k) \\ . & & . & & . \\ . & & . & & . \\ . & & . & & . \\ a_{N1}(r,k) & . & . & . & a_{NN}(r,k) \end{bmatrix} \quad (5)$$

for $r = 1,...,p$ and their elements are predicted utilizing the adaptive method given in Eq. 1-4. Based on that information, adaptive time-varying connectivity measures are defined on the following Z-transform of the MVAR parameters " $A_k^{(r)}$ " to the frequency domain as in Eq. 6.

$$A(k,f) = I - \sum_{r=1}^{p} A_k^{(r)} z^{-r} \Big|_{z=e^{j2\pi f}} \quad (6)$$

PDC, which is a time-varying connectivity measure, is defined in Eq. 7.[45,46]

$$\Pi_{ij}(k,f) \triangleq \frac{\left|A_{ij}(k,f)\right|^2}{\sum_{m=1}^{p}\left|A_{im}(k,f)\right|^2} \quad (7)$$

PDC quantifies the direct influence from time series to time series , after discounting the effect of all the other time series. The square exponents enhance the accuracy and stability of the estimates while the denominator part permits the normalization of outgoing connections by the inflows.[47]

Classification

Extracted features are then defined as input neurons to the classification algorithm. The output layer should include four neurons for the four classes that represent the four wrist movement states. The number of neurons in the input layer changes according to the length of the feature vector. NNs and SVMs play key roles in machine learning and data analysis. However, it is known that there exist some challenging issues with them such as intensive human intervention, slow learning speed, and poor learning scalability. In this article, we use ELM for the classification. ELMs are a kind of feedforward neural network, which does not necessitate gradient-based backpropagation for learning. It utilizes MP generalized inverse to set its weights. ELM not only learns up to tens of thousands faster than NNs and SVMs but also provides unified implementation for regression, binary, and multi-class applications. ELM is efficient for time series, online sequential, and incremental applications. ELM is also efficient for large datasets.

A single-hidden layer feedforward NN is shown in Figure 2.

The algorithm of a single-hidden layer feedforward NN can be listed as multiplication inputs by weights, adding bias,

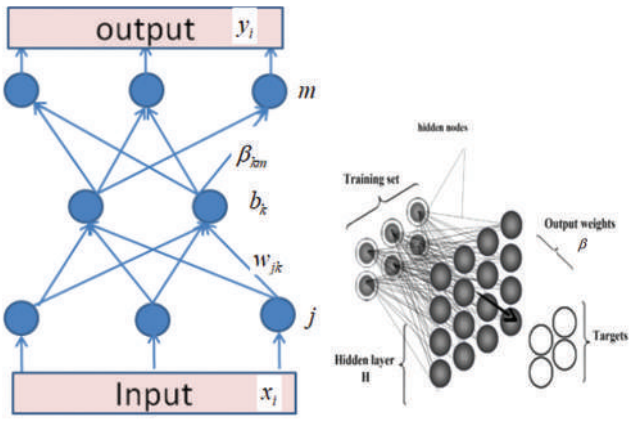

Figure 2: A generic single-hidden layer feedforward neural network architecture[48]

implementing the activation function, repeating the first three steps with a number of layers times, evaluating output, backpropagating, and repeating every step, respectively. The ELM differs from the feedforward NN by removing the repeating steps and replacing the backpropagation step with a matrix inverse operation.

The output of the ELM is evaluated as in Eq. 8.

$$f_L(x) = \sum_{i=1}^{L} \beta_i g_i(x) = \sum_{i=1}^{L} \beta_i g\left(w_i * x_j + b_i\right), j = 1,...,N \quad (8)$$

where L is the number of hidden units, N is the number of training samples, β_i is the weight vector between *ith* hidden layer and output, w is the weight vector between the input and hidden layer, $g(.)$ is an activation function, b is a bias vector, and x is an input vector.

β is a special matrix due to the pseudo-inverse operation. Eq. 8 can be represented in a compact form as in Eq. 9.

$$T = H\beta$$

$$H = \begin{bmatrix} g(w_1 * x_1 + b_1) & . & . & . & g(w_L * x_1 + b_L) \\ . & & . & & . \\ . & & . & & . \\ . & & . & & . \\ g(w_1 * x_N + b_1) & . & . & . & g(w_L * x_N + b_L) \end{bmatrix}_{N \times L}$$

$$\beta = \begin{bmatrix} \beta_1^T \\ . \\ . \\ . \\ \beta_L^T \end{bmatrix}_{L \times m}, T = \begin{bmatrix} t_1^T \\ . \\ . \\ . \\ t_N^T \end{bmatrix}_{N \times m} \quad (9)$$

where m is the number of outputs, H is called the hidden layer output matrix, and T is a training data target matrix.

Since there are no certain rules for choosing the number of hidden neurons, the EM-ELM method was used for finding the optimal configuration.

Machine interface design

JACO robotic arm, which is a generic 6-axis robotic manipulator with a three-fingered hand, can be used for the physical realization and machine interface of the proposed algorithm. The arm has six degrees of freedom in total with a maximum reach of 90 cm radius sphere and a maximum speed of 30 cm/s. It is made of three sensors: force, position, and acceleration. This arm should be suitable for a person with a disability of the upper arm and can be placed in a wheelchair. The upper arm of the robot is made of three links which are similar to the upper limb of the human body, as shown in Figure 3.

An API, which gives freedom of control to users, is provided by the manufacturers. The subject needs to control the movement of the robot arm toward a given target by using four mental commands: Forward (F), Backward (B), Left (L), Right (R), and No Movement command. To end the movement of the robot arm, the subject would generate a "No Movement" command by taking no action. The arm could move on two axes (x and y) and in four directions (forward (+y), backward (−y), left (+x), and right (−x)). The control signals are generated according to the mental commands. To move the arm forward, the subject imagines the forward wrist movement, and performs backward wrist movement to move the arm backward. The subject imagines moving his/her right wrist to move the robotic arm right and imagines moving his/her left wrist to move the robotic arm left. Forward differential kinematics gives the relation between joint velocities and tip velocity. This relation is in matrix form called Jacobian. To form Jacobian, first propagation matrices are created. The propagation matrix given in Eq. 10 produces the relation between sequenced joints.

$$\overline{\overline{V_b}} = \begin{bmatrix} \overrightarrow{w_b} \\ \overrightarrow{V_b} \end{bmatrix} = \begin{bmatrix} I & 0 \\ -\hat{l}_{ab} & I \end{bmatrix} \begin{bmatrix} \overrightarrow{w_a} \\ \overrightarrow{V_a} \end{bmatrix} + \begin{bmatrix} \vec{h} \\ \vec{0} \end{bmatrix} \dot{\theta}$$

$$\overline{\overline{V_b}} = \varphi_{ba} \overline{\overline{V_a}} + \overline{\overline{H}} \dot{\theta} \tag{10}$$

For fixed base manipulators, the robot propagation matrix can be constructed by using these joint relations. This matrix is called φ and gives all joint velocity vectors. To reach tip velocity, Eq. 11 should be evaluated.

$$\overline{\overline{V_t}} = \varphi_t \, \varphi \, H \underline{\dot{\theta}} \tag{11}$$

By using this equation, the robot tip velocity can be calculated concerning joint velocities. Hence, the Jacobian is given in Eq. 12.

$$J = \varphi_t \, \varphi \, H \tag{12}$$

MATLAB Simulink Code is created by using the above equations. First, the Jacobian is implemented, after that according to Rodrigues' formula, the rotation matrices for each joint are built. The coordinate frames for each joint change when the robot moves. For this reason, coordinate frames are updated at each sample time by using joint velocities, sample period, and rotation axes. However, this update mechanism is correct if the joint velocity is constant along the sample period. The selected sample time is 1 ms. The Simulink block diagram of the robot Jacobian is shown in Figure 4.

Inputs are base positions (6 × 1) and Robot Joint Angular Positions (6 × 1), and Outputs are Tip Point Position and Load Center Position. Tip and load center positions are fed to these shapes at the VRML file to confirm the operation of the moving base kinematic code. Only the angular part of the base position is used. These angles are Euler XYZ angles and converted to vector-angle representation and then fed to VRML file. Two common ways to create a dynamical model of a robot are Newton–Euler-based and Euler–Lagrange-based dynamical modeling. The Newton–Euler method, which is a vectorial approach, was explained in this article for dynamical modeling.

The dynamic model stated in Eq. 13 describes the relationship between joint forces and joint accelerations. The forces acting on a joint are the sequenced joint force and linear and angular inertia of the joint.

$$\overrightarrow{\tau_k} = \overrightarrow{\tau_{k+1}} + \overrightarrow{l_{k,k+1}} \times \overrightarrow{f_{k+1}} + \overrightarrow{l_{k,c}} \times \dot{\overrightarrow{v_k}} \, m_k + \frac{d}{dt} (I_k \overrightarrow{w_k})$$

$$\overrightarrow{f_k} = \overrightarrow{f_{k+1}} + m_k \frac{d}{dt} (\overrightarrow{v_k} + \overrightarrow{w_k} \times \overrightarrow{l_{k,c}}) \tag{13}$$

The compact form of Eq. 13 can be given as in Eq. 14.

$$\overline{\overline{F_k}} = \varphi_{(k+1,k)}^T \overline{\overline{F_{k+1}}} + M_k \dot{\overline{\overline{V_k}}} + \overline{\overline{b_k}}$$

$$M_k = \begin{bmatrix} I_k & m_k \hat{l}_{k,c} \\ -m_k \hat{l}_{k,c} & m_k I \end{bmatrix} \quad \dot{\overline{\overline{V_k}}} = \varphi_{k,k-1} \dot{\overline{\overline{V_{k-1}}}} + \overline{\overline{H_k}} \ddot{\theta}_k + \overline{\overline{a_k}}$$

$$\overline{\overline{b_k}} = \begin{bmatrix} \overrightarrow{w_k} \times I_k \overrightarrow{w_k} \\ m_k \overrightarrow{w_k} \times (\overrightarrow{w_k} \times \overrightarrow{l_{k,c}}) \end{bmatrix} \quad \overline{\overline{a_k}} = \begin{bmatrix} \overrightarrow{w_{k-1}} \times \overrightarrow{w_k} \\ \overrightarrow{w_{k-1}} \times (\overrightarrow{w_{k-1}} \times \overrightarrow{l_{k-1,k}}) \end{bmatrix} \tag{14}$$

If the robot joint dynamic equations are put together, Eq. 15 is obtained.

$$\underline{F} = \varphi^T (M(\dot{\underline{V}}) + \underline{b} + \varphi_t^T \overline{\overline{F_k}}) \tag{15}$$

Figure 3: JACO robotic arm mounted on an electric wheelchair[49]

Figure 4: Simulink block diagram of the robot Jacobian

The above equation includes all forces acting on the robot joints. To reach forces that make the robot joint accelerate, the force vector $\underline{F}$ is multiplicated with the rotation axis matrix as in Eq. 16.

$$\tau = H^T \underline{F} = \mu \ddot{\theta} + C + J^T F_t \quad (16)$$

Based on MATLAB kinematic code for moving base-robot systems, a dynamic model is built. The torque expressions are related to Jacobian terms. Because of that dynamic model code can be easily improved by starting with kinematic code. The first addition to kinematic code is creating μ the matrix according to base velocities, base accelerations, and fixed base dual robot "μ" The fixed base dual robot "μ" requires robot joint masses, inertia tensors, position vector of the center of mass, and joint angular velocity vectors. Masses, inertia tensors, and center of gravities concerning joint frames are found by investigating the SolidWorks drawing of the robot arm. Joint angular velocity vectors are provided from the previous iteration with zero initial points. After evaluating the fixed base "μ" the moving base features are added to the "μ" and a new "μ" is created. These additions are base mass matrix which depends on base mass, inertia tensor, the center of gravity, and base-robot mass matrices. C matrix is created based on H, φ, a vector, b vector, and mass matrix. After calculating these matrices, the forward dynamics of the robot with a moving base are simulated. Above torque, expression is prepared as torque input and acceleration output given in Figure 5 and Eq. 17.

$$\ddot{\theta} = \mu^{-1} (\tau - C - J^T F_t) \quad (17)$$

The inputs are Tip Forces (12 × 1), Base Forces (6 × 1), Joint Torques (12 × 1), and Joint Angular Velocity Vectors (12 × 1), respectively. The outputs are Accelerations (18 × 1), Tip Point Velocities (12 × 1), and Load Velocity (6 × 1), respectively.

Results

After applying the adaptive AR-based PDC feature extraction method to the train data matrix for each class, the time-variant estimated MVAR parameters were obtained. The size of the parameter vector for each class is 32000 × 200.The rows represent time in terms of data samples, and the columns show the parameter values estimated over samples. The most significant values of the adaptive PDC measures at a 99% level of significance after applying the surrogate data method are given in Figure 6 for each class of wrist movement states.

The adaptive PDC results show the connectivity between channels. It can be inferred from Figure 6 that the most significant direct coupling activities emerge from channel 3 to channels 1, 2, 4, and 5, respectively. The model parameters are accurately tracked and each class has different patterns.

The adaptive AR-based PDC feature matrices are concatenated and the feature train matrix is built, and the obtained train matrix is fed into the ELM. The size of the feature train matrix is 128000 × 200.

A principle component analysis-based dimension reduction algorithm, which is an orthogonal transformation constructing the relevant features, is applied to the feature train matrix because the number of extracted features is too much. The first four components having the most variance in the feature data are selected. After the dimensionality reduction process, the size of the feature train matrix becomes 128000 × 4.

The obtained data are randomly divided into training, testing, and validation sets. Every time the system is executed, samples were used for each task (70400 samples [55%] are used for training, 25,600 samples are used for validation [20%], and the remaining 32000 trials were used for the test [25%]). ELM has trained for 100 epochs (iterations) by incrementing the number of neurons in the hidden layer (hidden node). For each hidden node, the classification accuracy was evaluated in terms of the "root mean squared error" criteria. Figure 7 represents the performance curve sensitivity concerning the hidden node.

The rmse error approaches the equilibrium state while increasing the hidden nodes. Therefore, the number of hidden neurons is chosen as 100. The training ratio is selected using a trial and error process as 0.7. The activation function of the output layer is chosen as "sigmoid."

The confusion matrices are given in Figure 8.

Test data are used for the external validation process. The size of the reduced feature test matrix is 58400 × 4. After feeding the test data to the trained ELM model, the external validation accuracy of the ELM is found as 84.88%.

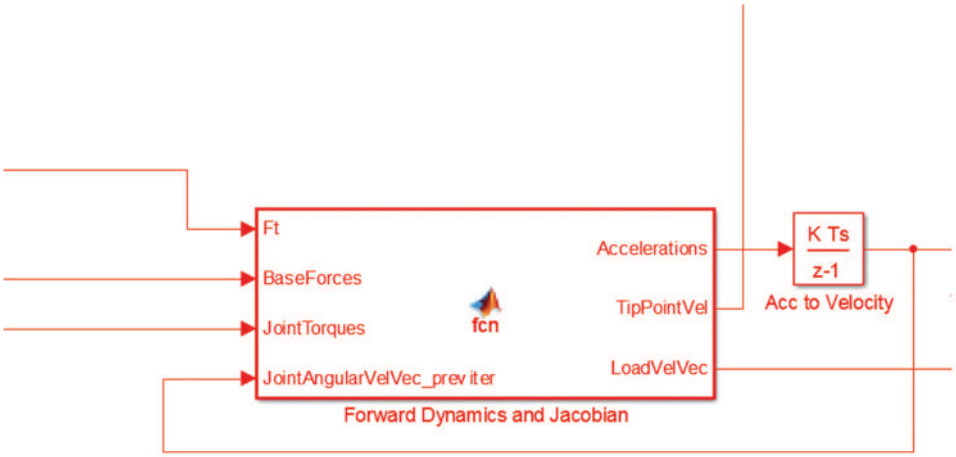

Figure 5: Simulink diagram of the forward dynamics

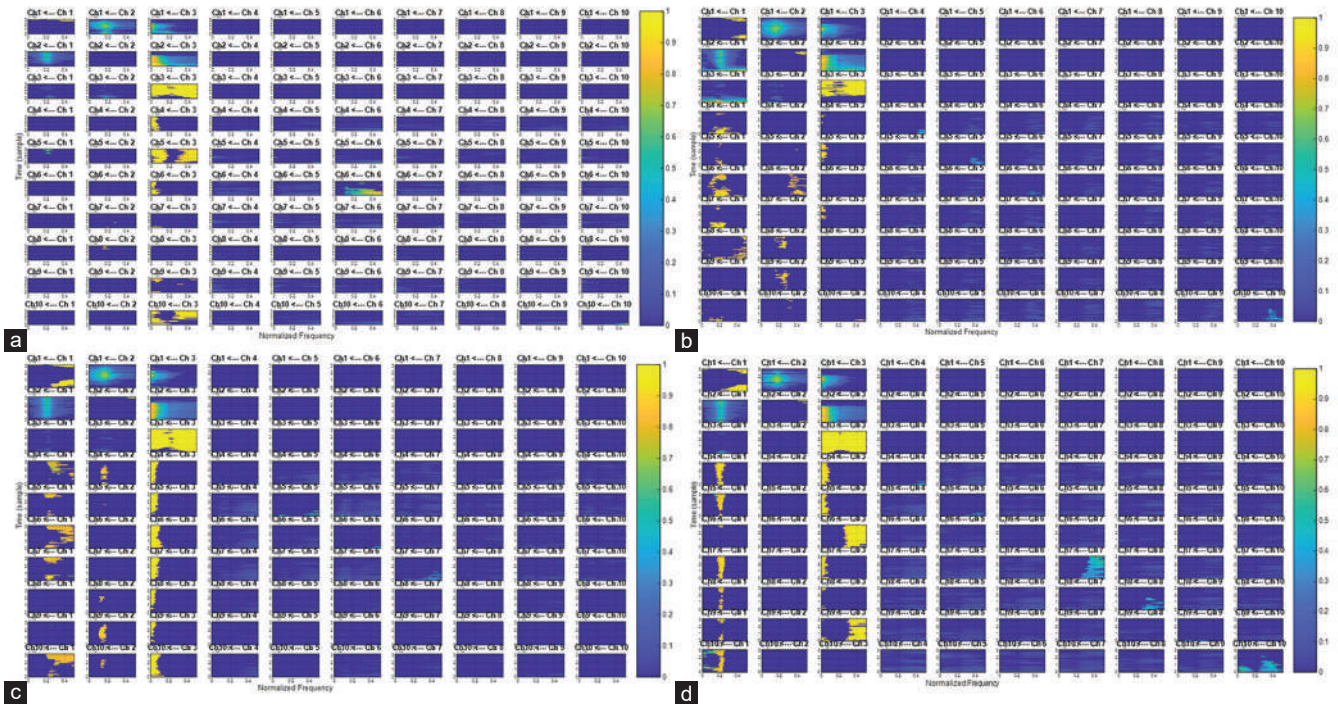

Figure 6: PDC for the simulated model utilizing the Kalman filtering approach. The x-axis represents normalized frequency ([0 0.5] corresponding to [0 0 F_s/2 and the y-axis represents the time direction in terms of data samples. Wrist movement states: (a) right, (b) forward, (c) left, and (d) backward. PDC: Partial directed coherence

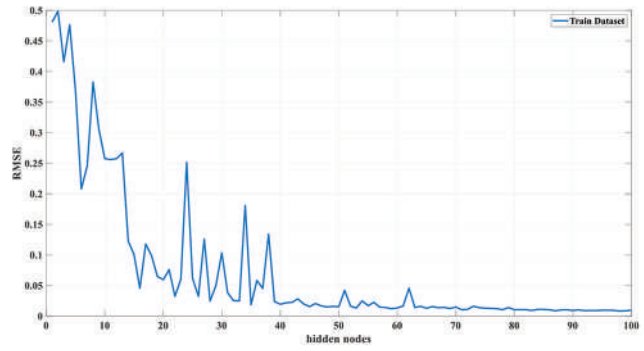

Figure 7: Hidden node selecting criteria

A comparative analysis was conducted over the external validation results using various classification methods and given in Table 1.

According to the external validation results, the ELM outperforms the other machine learning models, and also the computational speed is extremely fast.

Discussion and Conclusive Summary

The obtained results clarify that by applying the proposed methodology, control signals from an individual's MEG signals can control the robotic arm. Time-varying cortical neural connectivity features are

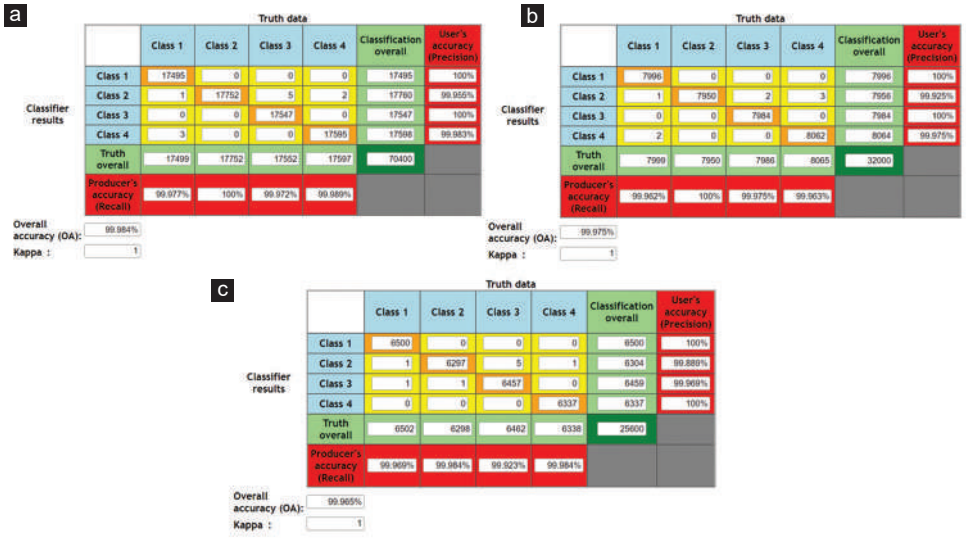

Figure 8: Confusion matrices: (a) training, (b) test, (c) validation. Class 1: right, Class 2: forward, Class 3: left, Class 4: backward

Table 1: Comparison of external validation classification results

Classifier	Sensitivity (%)	Precision (%)	Specificity (%)	F-measure (%)	Accuracy (%)
SVM	83.6	82.88	82.71	83.25	83.17
ELM	85.12	83.73	83.62	84.95	84.88
NB	75.45	77.03	76.74	76.23	76.08
k-NN	78.54	67.93	76.79	78.23	77.71
ANN	79.78	79.23	76.79	79.50	78.43

SVM: Support vector machine, ELM: Extreme learning machine, NB: Naive Bayesian, k-NN: k-nearest neighbor, ANN: Artificial neural network

strong biomarkers for characterizing the MEG patterns, which originated from wrist movements. According to the external validation classification results, ELM outperforms the other classifiers by achieving the highest accuracy. The accuracy of which these control signals are extracted from the MEG signals is extensively measured using the wide industry-employed receiver operator characteristic curves. After the signal processing part is taken care of, it is necessary to establish the dynamic model of the robot, create and simulate the solid model, eliminate the errors caused by the system dynamics in the robot joints, and synchronize with the brain signals. MEG-based BCI systems are capable to be robustly utilized as a control device through the proposed framework.

Patient informed consent

There is no need for patient informed consent.

Ethics committee approval

There is no need for ethics committee approval.

Conflicts of interest

There are no conflicts of interest to declare.

Financial support and sponsorship

No funding was received.

Author contribution subject and rate:

- Caglar Uyulan (100%): Design the research, data collection, and analyses and wrote the whole manuscript.

References

1. Mellinger J, Schalk G, Braun C, Preissl H, Rosenstiel W, Birbaumer N, *et al*. An MEG-based brain-computer interface (BCI). Neuroimage 2007;36:581-93. [Doi: 10.1016/j.neuroimage. 2007.03.019].
2. David G, Corral GH, Zentina LM. Using EEG / MEG data of cognitive processes in brain-computer interfaces. AIP Conf Proc 2008;1032:7. [Doi: 10.1063/1.2979300].
3. Çağlayan O, Arslan RB. Robotic arm control with brain computer interface using P300 and SSVEP. Biomed Eng 2013. p. 141-4. [Doi: 10.2316/p. 2013.791-082].
4. NandikollaV, Medina Portilla DA. Teleoperation robot control of a hybrid EEG-based BCI arm manipulator using Ros. J Rob 2022;2022:14. [Doi: 10.1155/2022/5335523].
5. Qasim M, Ismael OY. Shared control of a robot arm using BCI and computer vision. J Eur Syst Automat 2022;55:139-46. [Doi: 10.18280/jesa. 550115].
6. Musk E, Neuralink. An integrated brain-machine interface platform with thousands of channels. J Med Internet Res 2019;21:e16194. [Doi: 10.2196/16194].
7. Spüler M, Rosenstiel W, Bogdan M. Adaptive SVM-Based classification increases performance of a meg-based brain-computer interface (BCI). In: Artificial Neural Networks and Machine Learning – ICANN. Berlin, Heidelberg: Springer;

2012;7552:669-76. [Doi: 10.1007/978-3-642-33269-2_84].
8. Rezaei S, Tavakolian K, Nasrabadi AM, Setarehdan SK. Different classification techniques considering brain computer interface applications. J Neural Eng 2006;3:139-44. [Doi: 10.1088/1741-2560/3/2/008].
9. Corsi MC, Chavez M, Schwartz D, Hugueville L, Khambhati AN, Bassett DS. Integrating EEG and MEG signals to improve motor imagery classification in brain-computer interface. Int J Neural Syst 2019;29:12. [Doi: 10.1142/s0129065718500144].
10. Sabra NI, Abdel Wahed M. The use of meg-based brain computer interface for classification of wrist movements in four different directions. In: 2011 28th National Radio Science Conference (NRSC). Cairo, Egypt: IEEE; 2011. [Doi: 10.1109/nrsc. 2011.5873644].
11. Daliri MR. A hybrid method for the decoding of spatial attention using the meg brain signals. Biomed Signal Proc Control 2014;10:308-12. [Doi: 10.1016/j.bspc. 2012.12.005].
12. Scherer R, Vidaurre C. Motor imagery based brain-computer interfaces. Smart Wheelchairs Brain Comput Interfaces 2018. p. 171-95. [Doi: 10.1016/b978-0-12-812892-3.00008-x].
13. Uyulan C, Erguzel TT. Analysis of time – Frequency EEG feature extraction methods for mental task classification. Int J Comput Intell Syst 2017;10:1280. [Doi: 10.2991/ijcis. 10.1.87].
14. Uyulan C, Erguzel T. Comparison of wavelet families for mental task classification. J Neurobehav Sci 2016;3:59. [Doi: 10.5455/jnbs. 1454666348].
15. Sun L, Feng ZR. Classification of Imagery Motor EEG data with wavelet denoising and features selection. In: 2016 International Conference on Wavelet Analysis and Pattern Recognition (ICWAPR). Jeju, Korea (South): IEEE; 2016. [Doi: 10.1109/icwapr. 2016.7731641].
16. Murugappan M, Murugappan S Human emotion recognition through short time electroencephalogram (EEG) signals using fast fourier transform (FFT). In: 2013 IEEE 9th International Colloquium on Signal Processing and Its Applications. Kuala Lumpur, Malaysia: IEEE; 2013. [Doi: 10.1109/cspa. 2013.6530058].
17. Zaveri HP, Duckrow RB, Spencer SS. On the use of bipolar montages for time-series analysis of intracranial electroencephalograms. Clin Neurophysiol 2006;117:2102-8. [Doi: 10.1016/j.clinph. 2006.05.032].
18. Ludwig KA, Miriani RM, Langhals NB, Joseph MD, Anderson DJ, Kipke DR. Using a common average reference to improve cortical neuron recordings from microelectrode arrays. J Neurophysiol 2009;101:1679-89.
19. Mourino J, del R Millan J, Cincotti F, Chiappa S, Jane R, Babiloni F. Spatial filtering in the training process of a brain computer interface. In: 2001 Conference Proceedings of the 23rd Annual International Conference of the IEEE Engineering in Medicine and Biology Society. Istanbul, Turkey: IEEE; 2001. [Doi: 10.1109/iembs. 2001.1019016].
20. Saha PK, Rahman MA, Alam MK, Ferdowsi A, Mollah MN. Common spatial pattern in frequency domain for feature extraction and classification of multichannel EEG signals. SN Comput Sci 2021;2:11. [Doi: 10.1007/s42979-021-00586-9].
21. Uyulan C, Ergüzel TT, Tarhan N. Entropy-based feature extraction technique in conjunction with Wavelet packet transform for multi-mental task classification. Biomed Eng/Biomed Technik 2019;64:529-42. [Doi: 10.1515/bmt-2018-0105].
22. Güçlü U, Güçlütürk Y, Loo CK. Evaluation of fractal dimension estimation methods for feature extraction in motor imagery based brain computer interface. Procedia Comput Sci 2011;3:589-94. [Doi: 10.1016/j.procs. 2010.12.098].
23. Khadijah Nik AN, Yeon-Mo Y. Applying Kalman filter in EEG-based brain computer interface for motor imagery classification. In: 2013 International Conference on ICT Convergence (ICTC). Jeju, Korea (South): IEEE; 2013. [Doi: 10.1109/ictc. 2013.6675451].
24. Nicolas-Alonso LF, Gomez-Gil J. Brain computer interfaces, a review. Sensors (Basel) 2012;12:1211-79.
25. Madi MK, Karameh FN. Hybrid cubature kalman filtering for identifying nonlinear models from sampled recording: Estimation of neuronal dynamics. PLoS One 2017;12:e0181513.
26. Ma X. The research of brain-computer interface based on AAR parameters and neural networks classifier. In: Proceedings of 2011 International Conference on Computer Science and Network Technology. Harbin, China: IEEE; 2011. [Doi: 10.1109/iccsnt. 2011.6182491].
27. Nilesh R, Sunil W. Improving extreme learning machine through optimization a review. In: 2021 7th International Conference on Advanced Computing and Communication Systems (ICACCS). Coimbatore, India: IEEE; 2021. [Doi: 10.1109/icaccs51430.2021.9442007].
28. Lefebvre G, Cumin J. Recognizing human actions based on extreme learning machines. In: Proceedings of the 11th Joint Conference on Computer Vision, Imaging and Computer Graphics Theory and Applications. Italy: Roma; 2016. [Doi: 10.5220/0005675004780483].
29. Mukherjee H, Das S, Ghosh S, Obaidullah SM, Santosh KC, Das N, *et al.* A study on the extreme learning machine and its applications. In: Document Processing Using Machine Learning. ImprintChapman and Hall/CRC; 2019. p. 43-52. [Doi: 10.1201/9780429277573-4].
30. Matias T, Souza F, Araújo R, Gonçalves N, Barreto JP. On-line sequential extreme learning machine based on recursive partial least squares. J Process Control 2015;27:15-21. [Doi: 10.1016/j.jprocont. 2015.01.004].
31. Huang GB, Chen L, Siew CK. Universal approximation using incremental constructive feedforward networks with random hidden nodes. IEEE Trans Neural Netw 2006;17:879-92.
32. Rong HJ, Ong YS, Tan AH, Zhu Z. A fast pruned-extreme learning machine for classification problem. Neurocomputing 2008;72:359-66. [Doi: 10.1016/j.neucom. 2008.01.005].
33. Feng G, Huang GB, Lin Q, Gay R. Error minimized extreme learning machine with growth of hidden nodes and incremental learning. IEEE Trans Neural Netw 2009;20:1352-7. [Doi: 10.1109/tnn. 2009.2024147].
34. Silva DN, Pacifico LD, Ludermir TB. An evolutionary extreme learning machine based on group search optimization. In: 2011 IEEE Congress of Evolutionary Computation (CEC). New Orleans, LA, USA: IEEE; 2011. [Doi: 10.1109/cec. 2011.5949670].
35. Lan Y, Soh YC, Huang GB. Two-stage extreme learning machine for regression. Neurocomputing 2010;73:3028-38. [Doi: 10.1016/j.neucom. 2010.07.012].
36. Deng W, Zheng Q, Chen L. Regularized extreme learning machine. In: 2009 IEEE Symposium on Computational Intelligence and Data Mining. Nashville, TN, USA: 2009 IEEE Symposium on Computational Intelligence and Data Mining; 2009. [Doi: 10.1109/cidm. 2009.4938676].
37. X-jian D, X-guang L, Xu X. An optimization method of extreme learning machine for regression. In: Proceedings of the 31st Annual ACM Symposium on Applied Computing. 2016. p. 891-3 [Doi: 10.1145/2851613.2851882].
38. Ding S, Zhang N, Xu X, Guo L, Zhang J. Deep extreme learning machine and its application in EEG classification. Math Probl

Eng 2015;2015:1-11. [Doi: 10.1155/2015/129021].

39. Stosic D, Stosic D, Ludermir T. Voting based Q-generalized extreme learning machine. Neurocomputing 2016;174:1021-30. [Doi: 10.1016/j.neucom. 2015.10.028].
40. Omidvarnia AH, Mesbah M, Khlif MS, O'Toole JM, Colditz PB, Boashash B. Kalman filter-based time-varying cortical connectivity analysis of newborn EEG. Annu Int Conf IEEE Eng Med Biol Soc 2011;2011:1423-6.
41. Winterhalder M, Schelter B, Hesse W, Schwab K, Leistritz L, Klan D, *et al.* Comparison of linear signal processing techniques to infer directed interactions in multivariate neural systems. Signal Process 2005;85:2137-60. [Doi: 10.1016/j.sigpro. 2005.07.011].
42. Arnold M, Milner XH, Witte H, Bauer R, Braun C. Adaptive AR modeling of nonstationary time series by means of kalman filtering. IEEE Trans on Biomed Eng 1998;45:553-62. [Doi: 10.1109/10.668741].
43. Wang F, Balakrishnan V. Robust kalman filters for linear time-varying systems with stochastic parametric uncertainties. IEEE Trans Signal Process 2002;50:803-13. [Doi: 10.1109/78.992124].
44. Pagnotta MF, Plomp G, Pascucci D. A regularized and smoothed general linear kalman filter for more accurate estimation of time-varying directed connectivity(). Annu Int Conf IEEE Eng Med Biol Soc 2019;2019:611-5.
45. Pascucci D, Rubega M, Plomp G. Modeling time-varying brain networks with a self-tuning optimized kalman filter. PLoS Comput Biol 2020;16:e1007566.
46. Ghumare EG, Schrooten M, Vandenberghe R, Dupont P. A time-varying connectivity analysis from distributed EEG sources: A simulation study. Brain Topogr 2018;31:721-37.
47. UyulanC, de la Salle S, Erguzel TT, Lynn E, Blier P, Knott V, *et al.* Depression diagnosis modeling with advanced computational methods: Frequency-domain emvar and deep learning. Clin EEG Neurosci 2021;53:24-36. [Doi: 10.1177/15500594211018545].
48. Hu J, Zhang J, Zhang C, Wang J. A new deep neural network based on a stack of single-hidden-layer feedforward neural networks with randomly fixed hidden neurons. Neurocomputing 2016;171:63-72. [Doi: 10.1016/j.neucom. 2015.06.017].
49. Paul I, Ghosh S, Konar A. Voice Command decoding for position control of Jaco robot arm using a type-2 fuzzy classifier. In: 2020 IEEE International Conference on Electronics, Computing and Communication Technologies (CONECCT). Bangalore, India: IEEE; 2020. [Doi: 10.1109/conecct50063.2020.9198684].

Original Article

The Usage of Constrained Independent Component Analysis to Reduce Electrode Displacement Effects in Real-Time Surface Electromyography-Based Hand Gesture Classifications

Abstract

Aim: In real-time control of prosthesis, orthosis, and human–computer interface applications, the displacement of surface electrodes may cause a total disruption or a decline in the classification rates. In this study, a constrained independent component analysis (cICA) was used as an alternative method for addressing the displacement problem of surface electrodes. **Materials and Methods:** The study was tested by classifying six-hand gestures offline and in real-time to control a robotic arm. The robotic arm has five degrees of freedom, and it was controlled using surface electromyography (sEMG) signals. The classification of sEMG signals is realized using artificial neural networks. cICA algorithm was utilized to improve the performance of classifiers due to the negative effect of electrode displacement issues. **Results:** In the study, the classification results of the cICA applied and unapplied sEMG signals were compared. The results showed that the proposed method has provided an increase between 4% and 13% in classifications. The average classification rates for six different hand gestures were calculated as 96.66%. **Conclusions:** The study showed that the cICA method enhances classification rates while minimizing the impact of electrode displacement. The other advantage of the cICA algorithm is dimension reduction, which is important in real time applications. To observe the performance of the cICA in the real-time application, a robotic arm was controlled using sEMG signals.

Keywords: *Classifier, constrained independent component analysis, electrode, surface electromyography*

Ulvi Baspinar[1], Yahya Tastan[2], Huseyin Selcuk Varol[2]

[1]Faculty of Technology, Marmara University, [2]Institute of Pure and Applied Sciences, Marmara University, Istanbul, Turkey

Introduction

The concept of using prosthesis as a real limb for disabled persons or using muscle and limb movements to control giant robots may seem like a futuristic fantasy or science fiction novel, but the latest developments in biomedical,[1] biomechanics and sensor technology and commercially available prosthesis, such as i-Limb, Bebionics, Otto Bock's Genium Bionic prosthetic systems, and Thalmic Labs wearable gesture control systems, show that this concept is becoming a reality.

Despite these improvements, there are a number of issues that must be addressed. One of the obstacles in controlling prosthesis and in real-time human–computer interaction (HCI) applications are surface electromyography (sEMG) signals.[1] The sEMG signals are highly changeable signals. The signals can be affected by fatigue, artifacts, noise, and blood pressure. Beyond these parameters, electrode placement plays a vital role for high accuracy classifications.[2] While in motion, the prosthesis and the HCI devices' electrode places can be changed, and placing electrodes at the same point is very difficult.[3] Thus, the classification accuracy is either compromised or a retraining process is necessary. Hargrove *et al*. investigated how electrode displacement, size and orientation affect pattern recognition based on myoelectric control systems.[3] Hargrove *et al*. found that electrodes shifts, orientation, and size reduced classification accuracy by about 10%–30%.[3]

The issue with electrode displacement is that the classification algorithm is adjusted depending on a certain position

How to cite this article: Baspinar U, Tastan Y, Varol HS. The usage of constrained independent component analysis to reduce electrode displacement effects in real-time surface electromyography-based hand gesture classifications. J Neurobehav Sci 2022;9:107-13.

Ethics committee approval: There is no need for ethics committee approval.

Received : 04-12-2022
Accepted : 11-12-2022
Published : 29-12-2022

Orcid
Ulvi Baspinar {ORCID: 0000-0002-3359-9713}
Yahya Tastan {ORCID: 0000-0002-1170-113}
Huseyin Selcuk Varol {ORCID: 0000-0002-3968-4230}

Address for correspondence:
Mr. Ulvi Baspinar, Faculty of Technology, Marmara University, Istanbul, Turkey.
E-mail: ubaspinar@marmara.edu.tr

Access this article online

Website: www.jnbsjournal.com

DOI: 10.4103/jnbs.jnbs_34_22

Quick Response Code:

for a specific gesture. When the electrodes' positions are changed, the sEMG recordings are affected from the adjacent muscle activities, so classification rates decline. This problem can be described as a source separation of sEMG signals.

There are several studies in the literature for source separation. One of the source separation algorithms is independent component analysis (ICA). The use of ICA algorithms has become popular in removing artifacts, noise, and source separation of biomedical signals, such as electrocardiography, electroencephalography, and electromyography.[4] Although ICA provides a solution for source separation, it has disadvantages, such as finding the sources in a different order each time the algorithm is run.[5]

The ICA algorithm is used in several studies on hand gesture identification. Naik *et al.* proposed the identification of various hand gestures for HCI using ICA[6] and a multi-run ICA-based signal processing system for recognizing hand gestures with an artificial neural network (ANN) classifier.[7] They reported that ICA alone is not suitable for sEMG due to the nature of sEMG distribution and the disorder of the estimated sources. They classified three-hand gestures for HCI and six-hand gestures with high accuracy using four electrodes in two different studies.[8] Sueaseenak *et al*. classified eight gestures with 16 electrodes using an ICA classifier and compared the results with an ANN classifier.[9] They found the classification performances of the ICA classifier to be at 93.3%.

The constrained ICA (cICA) algorithm, which is a type of traditional ICA, can be used for the source separation applications in which any prior information about the source of interest is known. The purpose of the cICA algorithm is to obtain an output that is statistically independent from other sources and closest to the predefined reference signal. There are also studies of the source separation of biomedical signals that use the cICA algorithm.[10]

In this study, a constrained ICA solution is proposed for the displacement problem of electrodes, and the classification of six hand gestures (hand open-close, wrist flexion-extension, radial, and ulnar movement) was conducted offline with high accuracy using the estimated sEMG signals. The classification results of the cICA applied and unapplied sEMG signals were compared. The study shows that the proposed method also increases the classification performances of the ANN classifier. As an additional application, a robotic arm was controlled in real-time using sEMG signals. A simple task, which was gripping a cube and moving it to another place, was performed using hand gestures.

Materials and Methods

There is no need for ethics committee approval. In this section, robotic arm gestures for robotic arm control, electrode placement, data acquisition, signal processing methods, and the classification algorithms are discussed. The block diagram in Figure 1 illustrates the main steps in the study. The study can be divided into two sections. The first section is generating a demixing matrix, which is separating mixed sEMG signals in an offline operation.[7] The second section controlling the robotic arm in real time. While controlling the robotic arm, the demixing matrix is used first, which is obtained in the first step, and then the obtained estimated sEMG signals' features are extracted and classified to control the robotic arm.

Robotic arm and gestures for robotic arm control

In this study, the AX-12A Smart Robotic Arm (Crustcrawler, Inc., California) was chosen because its motion capability is similar to the commercially available prosthesis. It has five degrees of freedom. Six different hand gestures were used to control three degrees of the robotic arm.[8] These hand gestures were hand open-close, wrist flexion extension, and radial and ulnar deviations. In

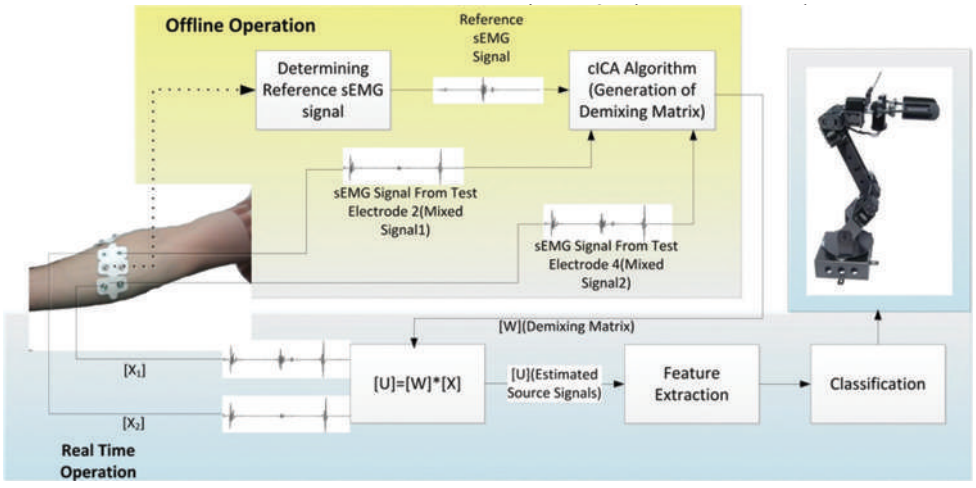

Figure 1: The block diagram of the cICA-based solution for the displacement problem of electrodes and the control of a robotic arm. cICA: Constrained independent component analysis

the controlling of the axis according to the gestures are shown.

Electrode placement and data acquisition

Electrode placement plays a vital role in sEMG-based systems. In this study, we used six electrodes. Two of them were cICA reference electrodes, and the other four electrodes were test electrodes. The cICA reference electrodes were placed along the longitudinal axes of the Brachioradialis and the Flexor Carpi Radialis muscles, respectively, and the other four electrodes were placed in parallel positions (25 mm away) to the ICA reference electrodes. The placements of the electrodes are shown in Figure 3. The bipolar passive disposable Ag/AgCL electrodes (Myotronics Inc., WA), which were 1 mm in diameter and 22 mm in interelectrode distance, were chosen for this study.

The analog sEMG signals were amplified using a homemade sEMG amplifier, and these amplified signals were converted to digital signals using the IOtech Personel Daq/3000 (IOTech, MA) series data acquisition system at 16 bits resolution with a 1 kHz sampling frequency.[11] The amplified sEMG signals were filtered using a band-pass filter, which allows for passing the signal between 20 Hz and 500 Hz.

Independent component analysis and constrained independent component analysis algorithm

ICA is a statistical method in which the goal is to decompose given multivariate data into a linear sum of statistically independent components. Recently, ICA has been used in the biomedical signals for removing artifacts, data reduction, and source separation.[12] The general ICA equation can be stated as in Eq 1 where S defines the source signal, A defines the unknown mixing matrix, X defines the mixture of source signals, W defines the unmixing matrix, and U defines the estimated source signals. The goal of ICA is to find a linear transformation W of the sensor signals X that makes the outputs U as independent as possible.[13] There are several algorithms to find the unmixing matrix W, and one algorithm is the Constrained ICA (cICA) algorithm.

$$[X] = [A] * [S]$$

$$[U] = [W] * [X]$$

Constrained ICA is an algorithm that searches statistically independent sources in mixed signals environments according to the predefined reference signal.[14] It is not necessary that this reference signal be the exact signal of interest. This knowledge is important because obtaining the perfect match for a reference signal is impossible in most cases. In studies that searched for a signal source in mixed environments, cICA is very useful because the conventional ICA finds sources in different orders, so it is difficult to determine whether or not the source of interest has been identified. So you cannot be sure it is the source that you are interested. The disadvantage of cICA is that the user must know the nature of the signal of interest to select the proper reference signal. In our study, the sEMG recordings of two electrodes were reduced to one sEMG signal according to a reference sEMG signal. The cICA model used in this study is depicted in Figure 4.

Reference surface electromyography selection

The success of the cICA algorithm completely depends on the selection of the reference signal.[15] The cICA algorithm cannot find the source signal of interest without obtaining the correct reference signal. In this study, the control of

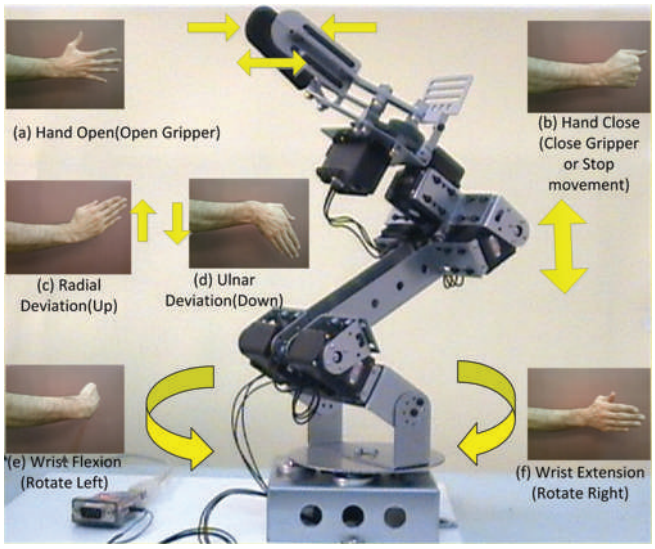

Figure 2: Hand gestures that were chosen for the control of the robotic arm and axis directions according to the gestures

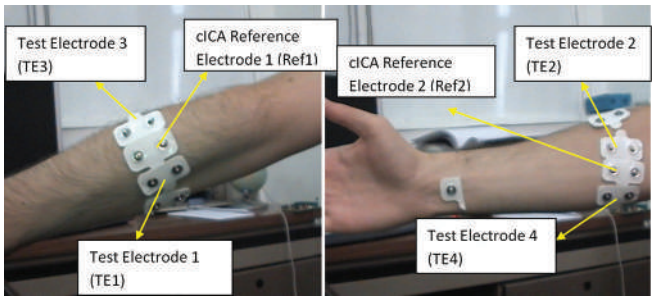

Figure 3: The placement of cICA reference electrodes and test electrodes. cICA: Constrained independent component analysis

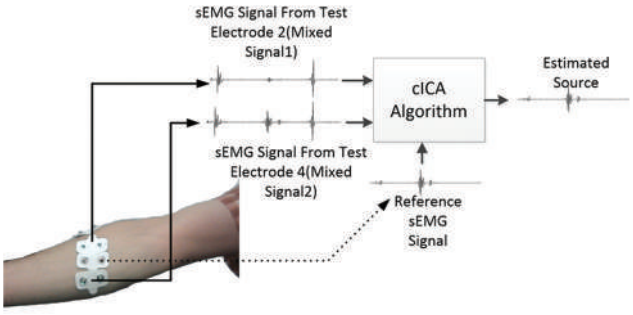

Figure 4: The constrained ICA model. ICA: Independent component analysis

the robot arm was performed using six-hand gestures, so twelve reference signals had to be determined for the six gestures recorded for the two muscles.

In order to determine the reference signals, the signals of the gestures were recorded first, while the subject was asked to perform six gestures and repeat the same gestures ten times. Second, the recorded sEMG signals' features were extracted.[16] Third, using these features, an ANN (12 neurons at the input layer, 20 neurons at the hidden layer, and 6 neurons at the output layer) was trained. Following the training session, the gestures with the minimum classification errors were recorded. The training process was repeated ten times, and the minimum misclassified gestures' signals were selected as reference signals.

Generating a demixing matrix

The cICA algorithm generates a demixing matrix using a reference signal in order to easily generate six demixing matrices for each gesture on one muscle and to use it for classification. The problem in this study was that we had to classify six gestures, but we did not know which gesture was detected before the real-time classification, which means that we could only use one demixing matrix for each muscle.[17] Our solution was to generate six demixing matrices using preselected reference signals and to calculate the medians of these six demixing matrices (demixing matrices are the same size) to get one common demixing matrix for one muscle. We used Brachioradialis and Flexor Carpi Radialis muscles to generate one demixing matrix for each muscle.

Feature extraction

The feature-extracting process is one of the most important parameters in classifying sEMG signals because it directly affects the classification performance. There are several feature-extracting methods for sEMG signals, but they are generally categorized as time and frequency domain features. In real-time systems, the frequency domain features are not preferred because of the extra time consumed in comparison with the time domain features. In this study, six-time domain features were used. These feature vectors are variance (Var), zero crossing, wavelength, Willison amplitude (WAmp), mean absolute value, and slope sign change.[18,19] Previous studies were considered in choosing the feature vectors.

Classification

The (ANN) is one of the most commonly used classification algorithms.[20] There are studies of the classification capability of ANN in sEMG signals.[21] The feedforward backpropagation ANN network type, which has one hidden layer with 20 neurons and one output layer with 6 neurons, is used in the study. The selected ANN has tansig and purelin activation functions at the hidden and output layers, respectively. While training the ANN, the Levenberg–Marquardt training algorithm and the mean squared error performance function were used. The classes of gestures were determined according to the majority voting result. When the gesture was detected, 1000 samples were recorded. The recorded gesture data were divided into five equal segments using a windowing technique as shown in Figure 5. Nonoverlapping windowing was used so that each window had 200 samples. For each segment, an ANN was trained so that means decisions were given according to the five ANNs. The results of the ANNs were evaluated using a majority voting algorithm, and the gesture with the highest vote was accepted as the winning gesture. The classifier model is depicted in Figure 6.

Results

This section is divided into two subsections: offline classification results and real-time control of the robotic arm.

Offline classification results

In this section, the results were compared according to the classification performances of cICA applied and unapplied sEMG signals, which were recorded in the vicinity of the reference points and evaluated based on the aspect of the classification of six-hand gestures using one and two muscles.[22]

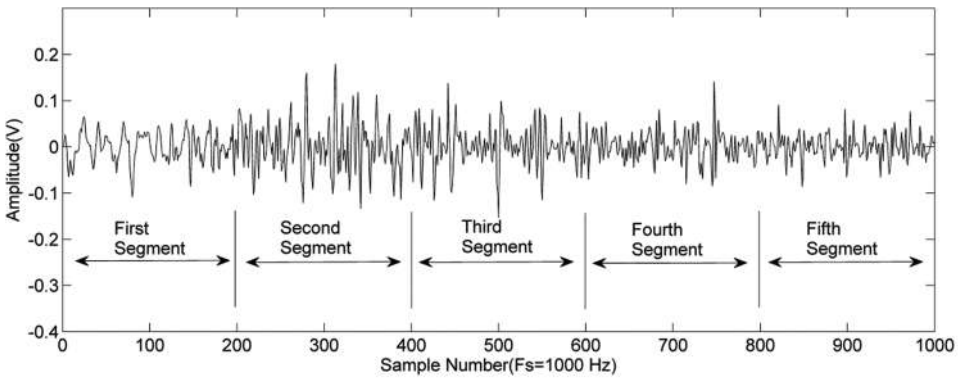

Figure 5: The segmentation of the recorded sEMG signal. sEMG: Surface electromyography

The ANN training process had random parameters to obtain more accurate classification results. Ten different ANNs with the same size were trained, and the classification results were recorded. In Table 1, the maximum, the minimum, and the calculated average values of the recorded classification results are shown.

First, we attempted to determine what would happen if we placed electrodes (TE1, TE2, TE3, and TE4) in the vicinity of the reference points (Ref 1 and Ref 2), as shown in Figure 3. The results show that the classification results declined up to 8% as expected. In other words, the reference points were chosen correctly.

Table 1: Classification results

Electrodes and cICA applied electrodes	Classification results (percentage)		
	Maximum	Minimum	Average
Ref1-Ref2	100	86.66	93
Ref1	90	76.66	83
Ref2	96.66	90	92.66
TE1	86.66	70	78.33
TE2	86.66	70	78.66
TE3	86.66	73.33	83
TE4	96.66	73.33	84
TE1-TE2-TE3-TE4	100	80	92.66
TE1-TE2	90	73.33	83
TE1-TE4	96.66	76.66	86.66
TE3-TE2	93.33	76.66	86.33
TE3-TE4	100	90	92.66
ESS1 (cICA applied to TE1-TE3)	93.33	76.66	89
ESS2 (cICA applied to TE2-TE4)	96.66	83.33	87.66
ESS1-ESS2	100	93.33	96.66

cICA: Constrained independent component analysis

Second, the classification effects of the cICA algorithm were investigated on the muscles Brachioradialis and Flexor Carpi Radialis, respectively. The TE1 and TE3 electrodes were placed in the vicinity of the Ref1 point on the Brachioradialis muscle, and the TE2 and TE4 electrodes were placed in the vicinity of the Ref2 point on the flexor carpi radialis muscle. The TE1-TE3 and TE2-TE4 signals were introduced to the cICA algorithm to obtain the ESS1 and ESS2 signals, respectively. The obtained ESS1 and ESS2 signals' effects on the average classification performances were calculated as 89% and 87.66%, respectively. These rates show a minimum increase of between 3% and 6% in classification performances when compared with the other electrodes, except the Ref1 and Ref2 electrodes.

Another evaluation was conducted regarding the cICA effect on the classification of six gestures when both of the muscles were included. When we generated the binary combination of the TE1, TE2, TE3, and TE4 electrodes on the two muscles, we obtained the TE1-TE2, TE1-TE4, TE3-TE2, and TE3-TE4 combinations. When we compared the effects of these generated binary combinations and ESS1-ESS2 with the classification results, an increase between 4% and 13% was observed. In

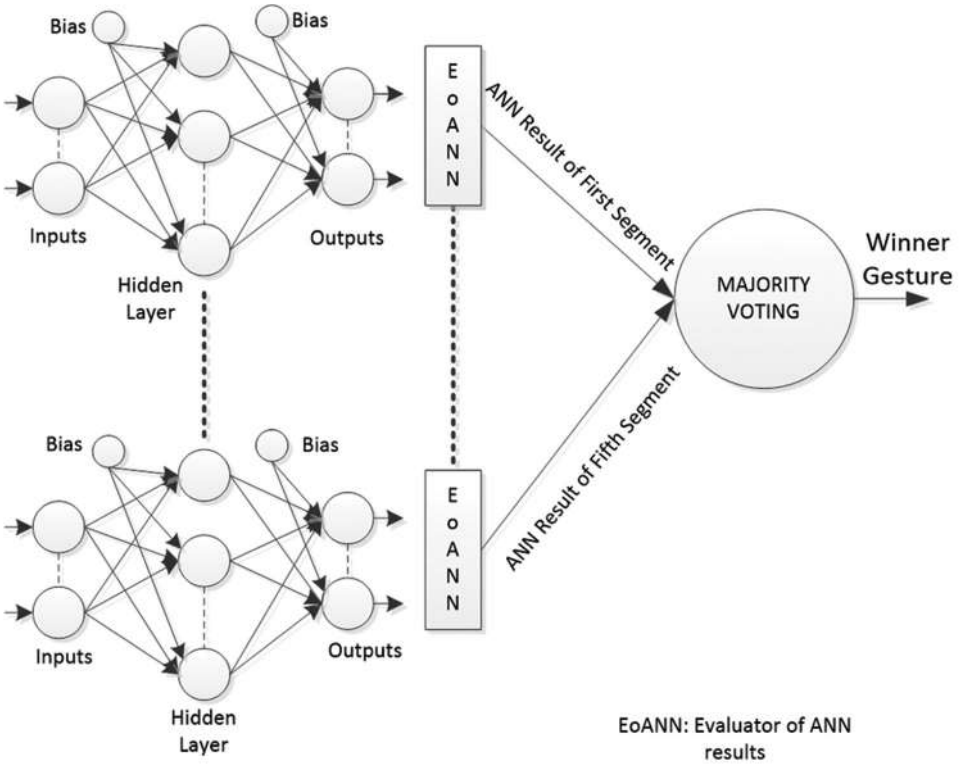

Figure 6: The ANN Classifier Model. ANN: Artificial neural network

addition [Figure 7], the comparison between ESS1-ESS2, Ref1-Ref2, and all electrodes (TE1-TE2-TE3-TE4) was made. The results indicate that when features of the ESS1-ESS2 signals are applied to the ANN classifier, the average success of the classifier increased to 96.66%, while the success rates of Ref1-Ref2 and TE1-TE2-TE3-TE4 were 93% and 92.66%, respectively.

Real-time control of the robotic arm

For real-time classification, four electrodes (TE1, TE2, TE3, and TE4) were used to estimate the sEMG signals (ESS1 and ESS2), as mentioned in the previous sections. The generation of reference signals, the demixing matrix calculation, and the training of the ANN were conducted offline, and the obtained demixing matrix, the network bias, and the layer weights were used in real-time classification. MATLAB software (version R2019a) was used for the calculation of the demixing matrix, the training of ANN, and the control of the robotic arm.[23] The communication and the control of the robot arm was carried out by the help of a PC, which has an AMD processor (2.80 Ghz) and 4.0 GB RAM, on a serial port. The classification duration of a gesture takes about 0.7 s after the motion is detected.

The sEMG signal was filtered with only a bandpass filter, which has the cut-off frequencies 20–500 Hz. There was no complex filtering technique applied to the raw data. The onset of sEMG signal activity was detected using the double-threshold method of *et al*.[24] This method operates on the raw myoelectric signal and does not require any envelope detection, so it is suitable for real time applications. A simple task was performed using an AX-12 robot arm. A small cube was placed on a desk, and the subject was asked to carry the cube to a target place using hand gestures. The subject moved the cube to the target place successfully. The photos taken during the real-time control of the robotic arm are shown in Figure 8.

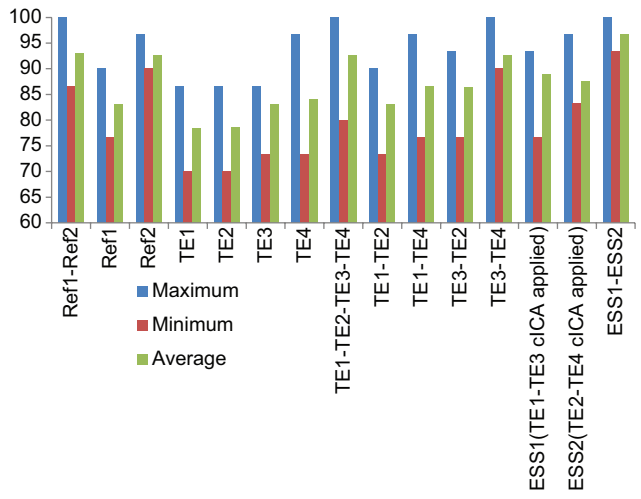

Figure 7: Performance comparison of sEMG signals recorded from reference points, cICA applied and unapplied electrodes. sEMG: Surface electromyography, cICA: Constrained independent component analysis

Discussion

This study shows that the cICA algorithm increases the classification accuracy while reducing the dimension and offers a solution to the problem of placing electrodes at the same reference point in real-time applications.

Dimension reduction offers an extra advantage, such as decreasing the computational load of the classifier, because it deals with fewer signals instead of all records. Unlike other techniques, the dimension reduction is as simple as multiplying input signals using a demixing matrix.

In addition, the classification of six gestures was realized in this study. The number of gestures can be increased to control the unused axis of the robotic arm, but placing extra electrodes on the related muscles may be necessary.

In the real-time experiments, we did not focus on the duration of the classification. Thus, 0.7 s seems long, but the duration can be minimized by using the optimization on the algorithm and running the algorithm on a specific embedded system, such as Field Programmable Gate Arrays.

The results of this study can be applied to other complex biomedical signals, such as EEG, in order to increase its classification in HCI applications and in the diagnosis of disorders.

Conclusions

The success of the cICA algorithm was tested both in the offline classification of hand gestures and in controlling a robot arm using six different hand gestures. The offline classification results show that cICA increased the classification performances to 96.6% while providing data reduction. In the second application, the robot arm was controlled with high accuracy. This study shows that the cICA algorithm can be applied as a solution to the displacement problem of electrodes in real-time applications.

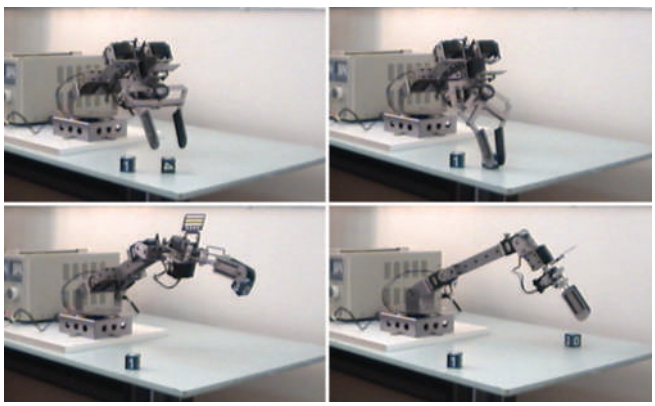

Figure 8: Real-time control of a robotic arm using hand gestures

Patient informed consent

Patient informed consent was obtained.

Ethics committee approval

There is no need for ethics committee approval.

Conflicts of interest

There are no conflicts of interest to declare.

Financial support and sponsorship

No funding was received.

Author contribution subject and rate

- Ulvi Baspinar (50%): Has conceived and designed the analysis, collected the data and performed the analysis.
- Yahya Tastan (25%): Wrote the paper, participated in its submission, and revised it.
- H.Selcuk Varol (25%): Has planned the study and revised the paper.

References

1. Hermens H, Hermanus J, Bart F. The State of the Art on Sensors and Sensor Placement Procedures for Surface Electromyography: A Proposal for Sensor Placement Procedures. Netherlands: Roessingh Research and Development; 1997.
2. Varol HA, Sup F, Goldfarb M. Multiclass real-time intent recognition of a powered lower limb prosthesis. IEEE Trans Biomed Eng 2010;57:542-51.
3. Hargrove L, Hudgins B, Englehart K, Leckey R. A comparison of surface and internally measured myoelectric signals for use in prosthetic control, engineering in medicine and biology society, 2006. EMBS'06. 28th Annual International Conference of the IEEE, IEEE, 2006. p. 2203-6.
4. Institute of Electrical and Electronics Engineers. Electrical Engineering Computing Science and Automatic Control (CCE), 2010 7th International Conference on : Date, 8-10 Sep. 2010. Institute of Electrical and Electronics Engineers; 2010.
5. Ibrahimy MI, Ahsan MR, Khalifa OO. Design and optimization of Levenberg-Marquardt based neural network classifier for EMG signals to identify hand motions. Meas Sci Rev 2013;13:142-51.
6. Naik GR, Kumar DK, Palaniswami M. Multi run ICA and Surface EMG Based Signal Processing System for Recognising Hand Gestures. Proceedings of the 8th IEEE International Conference on Computer and Information Technology (CIT 2008), 8-11 July 2008, Sydney, Australia. Published online 2008. p. 700-5.
7. Lu Z, Narayan A, Yu H. A deep learning based end-to-end locomotion mode detection method for lower limb wearable robot control. In: IEEE International Conference on Intelligent Robots and Systems. Las Vegas, NV, USA: Institute of Electrical and Electronics Engineers Inc.; 2020. p. 4091-7.
8. Stolyarov R, Carney M, Herr H. Accurate heuristic terrain prediction in powered lower-limb prostheses using onboard sensors. IEEE Trans Biomed Eng 2021;68:384-92.
9. Sueaseenak D, Wibirama S, Chanwimalueang T, Pintavirooj C, Sangworasil M. Comparison study of muscular-contraction classification between independent component analysis and artificial neural network. In: 2008 International Symposium on Communications and Information Technologies. Vientiane, Laos; ISCIT; 2008. p. 468-72.
10. Zhang ZL. Morphologically constrained ICA for extracting weak temporally correlated signals. Neurocomputing 2008;71:1669-79.
11. Park T, Lee M, Jeong T, Shin YI, Park SM. Quantitative analysis of EEG power spectrum and EMG median power frequency changes after continuous passive motion mirror therapy system. Sensors (Basel) 2020;20:2354. [Doi: 10.3390/s20082354].
12. Hussain T, Iqbal N, Maqbool HF, Khan M, Awad MI, Dehghani-Sanij AA. Intent based recognition of walking and ramp activities for amputee using sEMG based lower limb prostheses. Biocybern Biomed Eng 2020;40:1110-23.
13. Kim Y, Stapornchaisit S, Miyakoshi M, Yoshimura N, Koike Y. The effect of ICA and non-negative matrix factorization analysis for EMG signals recorded from multi-channel EMG Sensors. Front Neurosci 2020;14:600804.
14. Dai C, Hu X. Independent component analysis based algorithms for high-density electromyogram decomposition: Systematic evaluation through simulation. Comput Biol Med 2019;109:171-81.
15. Karimi F, Kofman J, Mrachacz-Kersting N, Farina D, Jiang N. Detection of movement related cortical potentials from EEG using constrained ICA for brain-computer interface applications. Front Neurosci 2017;11:356.
16. Grushko S, Spurný T, Černý M. Control methods for transradial prostheses based on remnant muscle activity and its relationship with proprioceptive feedback. Sensors (Basel) 2020;20:4883.
17. Zhou Y, Liu J, Zeng J, Li K. Sciences HLSCT, 2019 undefined. Bio-signal based elbow angle and torque simultaneous prediction during isokinetic contraction. Springer Sci. China Technol. Sci 2019;62:21-30. https://doi.org/10.1007/s11431-018-9354-5. Available from: https://link.springer.com/article/10.1007/s11431-018-9354-5. [Last accessed on 2022 Nov 27].
18. Abbaspour S, Lindén M, Gholamhosseini H, Naber A, Ortiz-Catalan M. Evaluation of surface EMG-based recognition algorithms for decoding hand movements. Med Biol Eng Comput 2020;58:83-100.
19. Khan AM, Sadiq A, Gul Khawaja S, Alghamdi NS, Akram MU, Saeed A. Physical action categorization using signal analysis and machine learning. arXiv preprint arXiv:2008.06971, 2020.
20. Basak H, Roy A, Lahiri JB. SVM and ANN based classification of EMG signals by using PCA and LDA Influenced by: Toward improved control of prosthetic fingers using surface electromyogram (EMG) signals. arXiv preprint arXiv:2110.15279, 2021.
21. Batayneh W, Abdulhay E, Alothman M. Prediction of the performance of artificial neural networks in mapping sEMG to finger joint angles via signal pre-investigation techniques. Heliyon 2020;6:e03669.
22. Copaci D, Arias J, Gómez-Tomé M, Moreno L, Blanco D. sEMG-based gesture classifier for a rehabilitation glove. Front Neurorobot 2022;16:750482.
23. Ligutan DD, Abad AC, Dadios EP. Adaptive Robotic Arm Control Using Artificial Neural Network. 2018 IEEE 10th International Conference on Humanoid, Nanotechnology, Information Technology, Communication and Control, Environment and Management, HNICEM; 2018. Published online March 12, 2019.
24. Bonato P, D'Alessio T, Knaflitz M. A statistical method for the measurement of muscle activation intervals from surface myoelectric signal during gait. IEEE Trans Biomed Eng 1998;45:287-99.

Original Article

NeuroPsychophysiological Investigation of ASMR Advertising Experience

Esil Sonmez Kence[1], Selami Varol Ülker[2], Sinan Canan[3]

[1]Department of Neuromarketing (Graduated), Üsküdar University Institute of Social Sciences, [2]Department of Psychology, Faculty of Humanities and Social Sciences, Üsküdar University, [3]Açıkbeyin Education and Consulting, Istanbul, Turkey

Abstract

Aim: The framework of this research is to examine the effects of autonomous sensory meridian responses (ASMRs) sensory/impulse circularity, psychological infrastructure, and the effects of brand advertisements using this technique on consumer behaviors and physiological outcomes such as product attitude, purchase intention, advertisement taste, and perceived visual advertisement esthetics. **Materials and Methods:** Mixed research method was used in the study, which consisted of consumers with high depressive mood and anxiety level (experimental group) and consumers with low depressive mood and anxiety level (control group). Electrodermal activity measurement and facial reading (facial coding) analysis are two specific neuromarketing research techniques utilized in this research. In addition, consumer attitude scales and psychological scales were employed. **Results:** According to the results obtained from the findings of the study, the physiological and attitudinal effects of ASMR advertisements do not show significant differences between the experimental and control groups. This is due to the fact that ASMR varies from person to person and has an atypical physiological pattern. **Conclusion:** The fact that ASMR is an ambiguous and contradictory experience with different physiological profiles due to factors such as causality, connectivity and relativity is consistent with the findings of this research.

Keywords: *Autonomous sensory meridian response, consumer neuroscience, consumer psychology, electrodermal activity, facial coding*

Introduction

Autonomous sensory meridian response (ASMR) is a sensory Internet phenomenon that arouses a certain sensation or feeling in its audience with audiovisual stimuli and has spread rapidly in recent years.[1,2] Scientifically, it is characterized by the progression of electrostatic-like tingling starting in the head-and-neck regions throughout the body from the spine line.[3,4] Many of the most popular ASMR videos feature, interpersonal triggers such as whispering and personal attention (e.g., haircuts) and nonperson-centered triggers such as crispy sounds and focused tasks (e.g., towel folding).[5]

In addition to the physical tingling sensation, researches and anecdotal texts in the field report that ASMR can be used as a therapeutic tool to help relax, struggle insomnia, feel calm, and relieve chronic pain and anxiety.[5-11] In this context, ASMR videos are "self-prescribed" by those who experience them as a method of regulating emotions and promoting sleep and healing.[12]

In the first academic study of the ASMR concept, it was stated that a significant portion of individuals with moderate and severe depression used ASMR videos to alleviate their depression or anxiety symptoms.[5] Another study examining whether ASMR is associated with differences in personality traits reports that individuals sensitive to ASMR score higher on empathic anxiety, daydreaming, and openness to experience than individuals who do not experience ASMR.[13]

Neuroscientific research on ASMR videos reports that individuals experiencing ASMR triggers show significant activation in brain regions associated with reward nucleus accumbens, sensory arousal dorsal anterior cingulate cortex, and social and emotional

How to cite this article: Kence ES, Ülker SV, Canan S. Neuropsychophysiological investigation of autonomous sensory meridian response advertising experience. J Neurobehav Sci 2022;9:114-20.

Ethics committee approval: The study protocol was approved by the Üsküdar University Non-Interventional Ethics Committee on February 25, 2022, with the number 61351342/2022-77.

Received : 15-11-2022
Revised : 13-12-2022
Accepted : 14-12-2022
Published : 29-12-2022

Orcid
Esil Sonmez Kence {ORCID: 0000 0001 9888 3371}
Selami Varol Ulker {ORCID: 0000 0002 6385 6418}
Sinan Canan {ORCID: 0000-0002-9864-1767}

Address for correspondence:
Esil Sonmez Kence, Barbaros Mah. Çiğdem Sok. Ağaoğlu Equinox B1 D:33 Ataşehir, İstanbul, Turkey. E-mail: esonmezkence@gmail.com

Access this article online

Website: www.jnbsjournal.com

DOI: 10.4103/jnbs.jnbs_32_22

Quick Response Code:

behavior (insula). Researchers, who observed significant brain activation in the region of the brain's medial prefrontal cortex associated with social behavior including self-awareness, social cognition, and care during ASMR, suggest that ASMR videos activate the brain similar to real social interaction.[14] In another study using the electroencephalography (EEG) technique, increased alpha activity was detected in the frontal and parietal regions of individuals with ASMR sensitivity compared to the control group.[15] Based on the fact that changes in alpha wave activity are generally associated with meditative processes;[16] the increased alpha wave activity detected by Fredborg *et al*. suggests that the ASMR experience creates a flow-like state, as in some forms of meditation.[15]

Other studies to test the physiological relevance of ASMR found statistically significant increases in pupil diameter with lower heart rate and increased skin conductance level measurements in participants.[11,17] The results of studies performed in the field show that ASMR is a contradictory experience with a different physiological profile, a mixed emotional structure, and a social component.[17]

The psychological infrastructure and sensory dimension of ASMR marketing which is expressed as "white noise" and "silent marketing," requires it to be examined in a whole with the fields of consumer psychology, consumer neuroscience, and consumer behavior. From this point of view, the attitudes and physiological reactions of consumers with high depressive mood and anxiety levels to advertising stimuli using the ASMR technique, which is stated to be calming and alleviate negative moods[5,18] are the focus of this research.

Materials and Methods

The study protocol was approved by the Üsküdar University Non Interventional Ethics Committee on February 25, 2022, with the number 61351342/2022 77.

Research design

In the study, the physiological effect of the independent variables (sensory stimuli included in ASMR-based advertisements) on the mediators (experimental and control groups) and their relationship with other dependent variables (advertising liking, product attitude, and purchase intention) are investigated. In this context, a mixed method consisting of two stages was designed. Research processes are given in Figures 1-3.

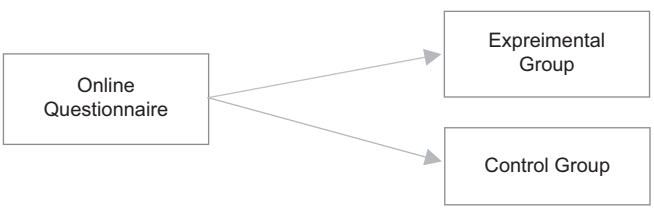

Figure 1: Mediators

Psychological measurements

In the first stage of the study, an online questionnaire is applied with the convenience sampling method. The questionnaire was built with Google Forms and designed in Turkish. The consent of the participants was obtained for the use of the data in the survey within the scope of the research. In the questionnaire, Beck Depression Inventory-II and Beck Anxiety Inventory-II were applied. Turkish validity and reliability of both inventories consisting of 21 items were made.[19,20] As a result of the online questionnaire, the participants are divided into two groups as high depressive mood/anxiety level (experimental group) and low depressive mood/anxiety level (control group).

Inclusion and exclusion criteria

Individuals (n = 173) who met the criteria for the 18–35 years age range (n = 162) were included in the online survey. Psychosomatic drug use was determined as the exclusion criterion (n = 151) to include individuals with high depressive mood and high anxiety levels in the study. Among the sampling group participating in the online survey, those residing outside of Istanbul (n = 131) were not included in the study as they could not participate in the experimental process conducted in the Üsküdar University Neuromarketing Laboratory.

Physiological measurements

The second stage of the study was started with the participants (n = 40) who declared that they would voluntarily participate in the research carried out at the Üsküdar University Neuromarketing Laboratory. Appointments were established within 10 days of the administration of the psychological scales.

In the laboratory, four ASMR advertisements from the automotive, food, beverage, and fashion sectors were watched and the neurophysiological reactions of the advertising stimuli were measured in both groups. Electrodermal activity (EDA) and face coding are two specific neuromarketing research techniques used in this research.

To measure the skin conductivity response, the iMotions Shimmer 3 GSR device is used. The device unit consists of an optical heart rate detection probe, optical heart rate sensors, GSR + electrodes, biophysical cables, and wrist strap. It has MSP430 microcontroller (24 MHz, MSP430

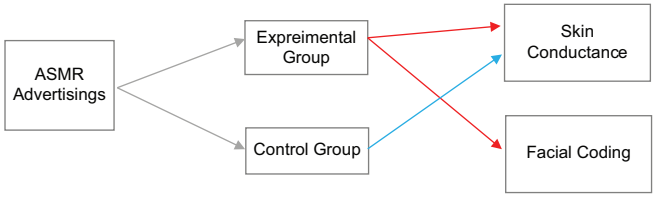

Figure 2: Physiological variables. ASMR: Autonomous sensory meridian response

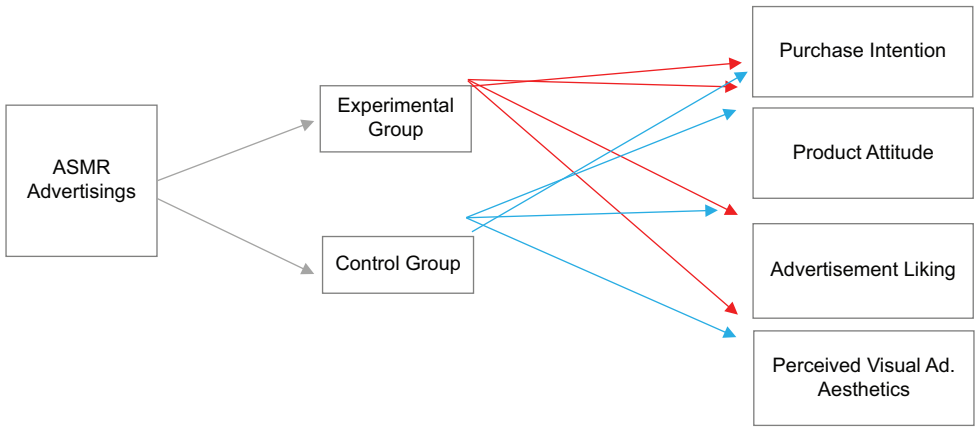

Figure 3: Variables of consumer attitude. ASMR: Autonomous sensory meridian response

CPU), Bluetooth radio (RN-42) integrated 2GB micro SD card, and 450 MAH installable lion battery. GSR level measurement range is 10k–4.7MΩ (0.2uS–100uS) ±10%. 22k–680kΩ (1.5–45uS) ±3%. During the experiment, two electrodes (Ag and AgCl surface electrodes) were placed on the second and third fingers of the participant's nondominant hand and the calibration was completed. The data obtained from the EDA device were analyzed by taking the peak point values.[21]

AFFDEX facial expression analysis module developed by iMotions was used in the research. The iMotions facial coding system identifies emotions by scanning facial expressions, regardless of environmental, contextual, or other factors.[22] A full HD Logitech brand camera, with 29 mm height, 94 mm width, and 24 mm depth, autofocusing at 1080p/30 fps–720/30 fps resolution, was used to obtain the correct face reading data of the individuals.

The calibrations of the participants were completed by sitting comfortably at a distance of 60 cm from the screen and camera. From the module, the participants' seven basic mood values (happiness, surprise, anger, sadness, humiliation, disgust, and fear) for each commercial film were analyzed over time percentage values.[23]

Consumer attitude

Consumer behavior in today's practice has a psychological background. When it comes to the process of examining consumer behaviors and psychological states, it is understood that examining the effects of depression, which is widely seen today, on consumer behavior is an important research topic.[24] As a matter of fact, in this study, experimental and control groups are determined according to depression and anxiety scales, and their attitudes that occur when they are exposed to ASMR-based advertising videos are investigated through consumer neuroscience measurements.

To correlate the sensory perception of the participants with the brand marketing performance indicators, they were asked to answer the survey questions using the scales of purchase intention, product attitude, advertisement liking, and perceived visual advertisement esthetics for four commercials.

The design of the study is shown in Table 1.

Results

The effects of stimulants on independent variables in experimental and control group contrast were analyzed using the Mann–Whitney *U*-Test.

Results of facial coding measurement

In the study, seven basic emotions, anger, sadness, disgust, happiness, surprise, fear, and humiliation, were analyzed based on four different commercials in contrast to the experimental and control groups. The microexpressions that occur while watching commercials in the food, automotive, beverage, and fashion industries are given in the tables [Tables 2-5].

As seen in Table 2, the scores of seven emotions obtained from the face reading measurement of the food brand commercial film did not show a statistically significant difference between the experimental and control groups ($P > 0.05$).

As seen in Table 3, the scores of seven emotions obtained from the face reading measurement of the automotive brand commercial film did not show a statistically significant difference between the experimental and control groups ($P > 0.05$).

As seen in Table 4, the scores of seven emotions obtained from the face reading measurement of the beverage brand commercial film did not show a statistically significant difference between the experimental and control groups ($P > 0.05$).

As seen in Table 5, the scores of seven emotions obtained from the face reading measurement of the fashion brand commercial film did not show a statistically significant difference between the experimental and control groups ($P > 0.05$).

Table 1: Research design

Mediators	Type of influence
ASMR	Physiological – Behavioral
Advertisings	
Experimental group	Condition 1 – Condition 2
Control group	Condition 3 – Condition 4

ASMR: Autonomous sensory meridian response

Table 2: Food brand facial coding measurement

Facial Coding	Group	*n*	±SD	*Z*	*P*
Anger TP	Control	20	0.00±0.00	-	1.000
	Experiment	20	0.00±0.00		
Sadness TP	Control	20	0.00±0.00	-	1.000
	Experiment	20	0.00±0.00		
Disguss TP	Control	20	0.00±0.00	-	1.000
	Experiment	20	0.00±0.00		
Joy TP	Control	20	4.37±11.4	-0,344	0.731
	Experiment	20	4.33±12.41		
Surprise TP	Control	20	0.00±0.00	-	1.000
	Experiment	20	0.00±0.00		
Fear TP	Control	20	0.04±0.17	-1.000	0.317
	Experiment	20	0.00±0.00		
Contempt TP	Cotrol	20	0.00±0.00		1.000
	Experiment	20	0.00±0.00		

TP: Time Percentage, SD: Standard Deviation

Table 3: Automotive brand facial coding measurement

Facial Coding	Group	*n*	±SD	*Z*	*P*
Anger TP	Control	20	0.03±0.12	-1.000	0.317
	Experiment	20	0.00±0.00		
Sadness TP	Control	20	0.00±0.00	-	1.000
	Experiment	20	0.00±0.00		
Disguss TP	Control	20	0.19±0.77	-1.065	0.287
	Experiment	20	0.01±0.05		
Joy TP	Control	20	0.37±1.45	-1,432	0.152
	Experiment	20	0.00±0.00		
Surprise TP	Control	20	0.02±0.07	-1.000	0.317
	Experiment	20	0.00±0.00		
Fear TP	Control	20	0.28±0.72	-1.777	0.076
	Experiment	20	0.00±0.00		
Contempt TP	Control	20	0.04±0.17	-1.000	0.317
	Experiment	20	0.00±0.00		

TP: Time Percentage, SD: Standard Deviation

Results of electrodermal activity measurement

By taking the peak point values from the EDA device, the data of the control and experimental groups were analyzed with the Mann–Whitney *U*-Test. The table [Table 6] contains data on EDA and heart rate measurement data according to the order of advertisement viewing.

As seen in Table 6, the peak level and black page scores obtained from the skin conductivity measurement of the food, automotive, beverage, and fashion brands did not show a statistically significant difference between the experimental and control groups ($P > 0.05$).

Results of consumer attitude measurement

Evaluation of consumer attitude scales was carried out with a 5-point Likert scale. There was no statistically significant difference ($P > 0.05$) between the experimental ($n = 20$) and control groups ($n = 20$) in the parameters of product attitude, advertisement likes, perceived visual advertisement esthetics, and purchase intention.

Discussion

The EDA and face coding analyses measured while watching the commercials of the participants showed that there was no statistically significant difference ($P > 0.05$) between the experimental group ($n = 20$) and the control group ($n = 20$).

In a study using an eye-tracking technique, the detection of statistically significant increases in pupil diameter while watching an ASMR video showed the stimulating aspect of ASMR; in another ASMR study using the EEG technique, the detection of increased alpha waves in the frontal and parietal regions reveals that ASMR is associated with mediative processes.[15] This suggests that the stimulating as well as calming and physiological outcomes[17] of ASMR may be atypical.

Moreover, it coincides with ASMRs "not for all-aspect" claim.[25] The fact that ASMR is an uncertain and contradictory experience with different physiological profiles due to factors such as causality, connectivity, and relativity is consistent with the results of this research.[11,26]

In addition, in group data of EDA, it is seen that there are extreme individual value differences in our study. In this situation, as stated above, the fact that ASMR advertisements have an atypical physiological pattern supports the view that ASMR can be stimulating as well as pleasant and calming.[17]

In our research, consumer attitude parameters were measured with a 5-point Likert evaluation, in the rating between "1 = I strongly disagree" and "5 = I strongly agree." The hypothesis that the experimental group would give a positive value compared to the control group based on the depression and anxiety-relieving properties of ASMR in the relevant parameters did not differ statistically in the findings. This is consistent with the fact that Elgün *et al*. revealed that there is no significant cause–effect relationship between depression and consumer styles.[24]

However, it was observed that the experimental and control groups had an average of three points or more in consumer attitude scales. The fact that the evaluation average of the stimuli is above the scores of "1 = strongly disagree" and "2 = disagree" can be explained by the view that when sensory properties are added to the brand

Table 4: Bevereage brand facial coding measurement

Facial Coding	Group	*n*	±SD	*Z*	*P*
Anger TP	Control	20	0.12±0.55	-1.000	0.317
	Experiment	20	0.00±0.00		
Sadness TP	Control	20	0.00±0.00	-	1.000
	Experiment	20	0.00±0.00		
Disguss TP	Control	20	0.06±0.17	-1.432	0.152
	Experiment	20	0.00±0.00		
Joy TP	Control	20	1.87±6.94	-0,827	0.408
	Experiment	20	0.42±1.56		
Surprise TP	Control	20	0.00±0.00	-	1.000
	Experiment	20	0.00±0.00		
Fear TP	Control	20	0.04±0.17	-1.000	0.317
	Experiment	20	0.00±0.00		
Contempt TP	Control	20	0.00±0.00	-	1.000
	Experiment	20	0.00±0.00		

TP: Time Percentage, SD: Standard Deviation

Table 5: Fashion brand facial coding measurement

Facial Coding	Grup	*n*	±SD	*Z*	*P*
Anger TP	Control	20	0.01±0.02	-1.000	0.317
	Experiment	20	0.00±0.00		
Sadness TP	Control	20	0.00±0.00	-	1.000
	Experiment	20	0.00±0.00		
Dısgus TP	Control	20	0.00±0.00	-	1.000
	Experiment	20	0.00±0.00		
Joy TP	Control	20	0.11±0.5	-0,651	0.515
	Experiment	20	0.86±2.84		
Surprise TP	Control	20	0.04±0.2	-1.000	0.317
	Experiment	20	0.00±0.00		
Fear TP	Control	20	0.01±0.05	-1.000	0.317
	Experiment	20	0.00±0.00		
Contempt TP	Control	20	0.05±0.22	-1.000	0.317
	Experiment	20	0.00±0.00		

TP: Time Percentage, SD: Standard Deviation

Table 6: Contrast of skin conductivity measurement

Skin Conductivity	Group	*n*	±SD	*Z*	*P*
Food Brand Peak Count	Control	20	1.55±2.58	-0.291	0.771
	Experiment	20	1.00±1.92		
Food Brand Black Page	Control	20	0.05±0.22	-1.041	0.298
	Experiment	20	0.15±0.37		
Automotive Brand Peak Count	Control	20	1.30±2.11	0.125	0.995
	Experiment	20	1.85±3.13		
Automotive Brand Black Page	Control	20	0.05±0.22	-1,066	0.287
	Experiment	20	0.30±0.92		
Beverage Brand Peak Count	Control	20	1.90±2.94	-0.291	0.771
	Experiment	20	1.65±3.41		
Beverage Brand Black Page	Control	20	0.10±0.31	-	1.000
	Experiment	20	0.10±0.31		
Fashion Brand Peak Count	Control	20	1.85±2.78	-0.489	0.625
	Experiment	20	2.45±3.65		
Fashion Brand Black Page	Control	20	0.10±0.31	-0.472	0.637
	Experiment	20	0.15±0.37		

SD: Standard Deviation

stimulus, positive emotion is induced in the consumer without requiring cognitive effort.[27] In this context; ASMR-based advertisements can have a positive effect on individuals who experience differences in anxiety level and depressive mood, regardless of the consumer psychology factor.

Limitations

Due to the significant relationship between gender role and psychological help-seeking,[28] the male experimental group's participation in the study was limited and the gender distribution in the study sample could not be kept equal. For this reason, the study was carried out with female participants, which constitutes one of the main limitations of the study. The fact that the study consisted of two periods and that the participants were invited to the laboratory stage during the pandemic process was restrictive, so it was followed by convenience sampling. The research was carried out among Üsküdar University undergraduate and graduate students.

The homogeneity of the sociodemographic structure constitutes one of the limitations of the research since it has a sample free from different effects. Heterogeneous studies are important in terms of reflecting the elements in the research universe to the sample.[29]

Future researches

In this study, no significant difference was found in physiological reactions between the experimental and control groups. Future studies may design detailed multidisciplinary studies in consumer neuroscience, consumer psychology, and marketing.

Depending on the association of the ASMR concept with an atypical physiological pattern and the results of our research supporting this relationship, future studies can be fed from additional physiological measurements to EDA and face reading analyzes. To obtain different outputs in physiological reactions to sensory stimuli, they can include especially pupil and Photoplethysmogram (PPG) data in their research.

Considering the psychological dimension of the research, adding personality inventories and attention awareness scales to the research in addition to psychological inventories, based on the connectivity between ASMR and personality factors, will add significance to neuromarketing research.

As far as is known, no research has been conducted in the literature on ASMR marketing using the neuropsychophysiological mixed method. In this context, the results of the research can help future studies to develop new methodologies for neuromarketing research that takes into account psychological factors to meet the needs and emotions of real consumers and to examine ASMR marketing, which has a place in the field of sensory marketing.

Multidisciplinary studies investigating the specific forms of consumers – especially benefiting from neuroscience and psychology disciplines – will contribute to the understanding of consumer behavior and literature.

Patient informed consent

Patient informed consent was obtained.

Ethics committee approval

The study protocol was approved by the Üsküdar University Non-Interventional Ethics Committee on 25/02/2022 with the number 61351342/2022-77.

Financial support and sponsorship

No funding was received.

Conflicts of interest

There are no conflicts of interest to declare.

Author contribution subject and rate

- Esil Sonmez Kence (%50): Design the research, data collection and analyses and wrote the whole manuscript.
- Dr. Selami Varol Ulker (%30): Organized the research and supervised the article write-up.
- Prof. Dr. Sinan Canan (%20): Contributed with comments on manuscript organization and write-up.

References

1. Kim B. ASMR in Advertising and its Effects: The Moderating Role of Product Involvement and Brand Familiarity (Doctoral Dissertation Texas, Austin: The University of Texas at Austin; 2020. [Doi: 10.26145/tsw/1013].
2. Smith SD, Katherine Fredborg B, Kornelsen J. An examination of the default mode network in individuals with autonomous sensory meridian response (ASMR). Social neuroscience 2017;12:361-5. [doi: 10.1080/17470919.2016.1188851].
3. Barratt EL, Spence C, Davis NJ. Sensory determinants of the autonomous sensory meridian response (ASMR): Understanding the triggers. PeerJ 2017;5:e3846. [Doi: 10.7717/peerj. 3846].
4. Fredborg BK, Clark JM, Smith SD. Mindfulness and autonomous sensory meridian response (ASMR). PeerJ 2018;6:e5414. [Doi: 10.7717/peerj. 5414].
5. Barratt EL, Davis NJ. Autonomous sensory meridian response (ASMR): A flow-like mental state. PeerJ 2015;3:e851. [Doi: 10.7717/peerj. 851].
6. Long R. Why are Whispering Videos so Popular on YouTube? The Quiet World of ASMR. Medium 2017. Available from https://medium.com/creative-landscape-of-youtube/why-are-whispering-videos-so-popular-on-youtube-the-quiet-world-of-asmr-27e0e9e62b49. [Last accessed on 2022 Oct 05].
7. Lopez, G. ASMR, explained: why millions of people are watching YouTube videos of someone whispering. Vox; 2018. Available from https://www.vox.com/2015/7/15/8965393/asmr-video-youtube-autonomous-sensory-meridian-response. [Last accessed on 2022 Jul 19].
8. Messitte, N. Is there any money to be made in ASMR? Forbes 2015. Available from https://www.forbes.com/sites/nickmessitte/2015/03/31/is-there-any-money-to-be-made-in-asmr/?sh=2a1e40c44e08. [Last accessed on 2022 Jun 23].
9. Hostler TJ, Poerio GL, Blakey E. Still more than a feeling: Commentary on Cash *et al.*, Expectancy effects in the autonomous sensory meridian response and recommendations for measurement in future ASMR research. PeerJ 2018;6:e5229. [Doi: 10.7717/peerj. 5229].
10. Richard C. Brain Tingles: The Secret to Triggering Autonomous Sensory Meridian Response for Improved Sleep, Stress Relief, and Head-to-toe Euphoria: Simon and Schuster: Avon MA; 2018.
11. Valtakari NV, Hooge IT, Benjamins JS, Keizer A. An eye-tracking approach to autonomous sensory meridian response (ASMR): The physiology and nature of tingles in relation to the pupil. PLoS One 2019;14:e0226692. [Doi: 10.1371/journal.pone. 0226692].
12. Poerio GL, Mank S, Hostler TJ. The awesome as well as the awful: Heightened sensory sensitivity predicts the presence and intensity of autonomous sensory meridian response (ASMR). J Res Pers 2022;97:104183. [Doi: 0.1016/j.jrp. 2021.104183].
13. Janik McErlean AB, Banissy MJ. Assessing individual variation in personality and empathy traits in self-reported autonomous sensory meridian response. Multisens Res 2017;30:601-13. [Doi: 10.1163/22134808-00002571].
14. Lochte BC, Guillory SA, Richard CAH, Kelley WM. An fMRI investigation of the neural correlates underlying the autonomous sensory meridian response (ASMR). Bioimpacts 2018;8:295-304. [Doi: 10.15171/bi. 2018.32].
15. Fredborg BK, Champagne-Jorgensen K, Desroches AS, Smith SD. An electroencephalographic examination of the autonomous sensory meridian response (ASMR). Conscious Cogn 2021;87:103053. [Doi: 10.1016/j.concog. 2020.103053].
16. Aftanas LI, Golocheikine SA. Human anterior and frontal midline theta and lower alpha reflect emotionally positive state and internalized attention: High-resolution EEG investigation of meditation. Neurosci Lett 2001;310:57-60. Doi: 10.1016/S0304-3940(01)02094-8].
17. Poerio GL, Blakey E, Hostler TJ, Veltri T. More than a feeling: Autonomous sensory meridian response (ASMR) is characterized by reliable changes in affect and physiology. PLoS One 2018;13:e0196645. [Doi: 10.1371/journalpone. 0196645].
18. Richard C. ASMR Research Project. ASMR Online University;2014. Available from https://asmruniversity.com/asmr-survey/. [Last accessed on 2022 Apr 10].
19. Hisli N. Beck depresyon envanterinin geçerliliği üzerine bir çalışma (a study on the validity of beck depression inventory.). Psikoloji Derg 1988;6:118-22.
20. Ulusoy M. Beck Anksiyete Envanteri: Geçerlik ve güvenirlik çalışması. Uzmanlık tezi. İstanbul: Bakırköy Prof. Dr. Mazhar Osman Mental Health and Neurological Diseases Training and Research Hospital; 1993.
21. Nikula R. Psychological correlates of nonspecific skin conductance responses. Psychophysiology 1991;28:86-90.
22. Ülker SV, Sayar GH. An investigation of biological markers of adult attachment in the framework of polyvagal theory. Int J Soc Sci Hum Res 2022;5:507-18. [Doi: 10.47191/ijsshr/v5-i2-16].
23. Facial Expression Analysis: The Definitive Guide; 2016. Available from https://imotions.com/support/document-library/. [Last accessed on 2022 Noa 07].
24. Elgün MN, Karabiyik HÇ, Kaleci F. Understanding the depressed consumer: A quantitative study on the consumption patterns of individuals in depression. Third Sector Soc Econ Rev 2021;1:451-69. [Doi: 10.15659/3. sektor-sosyal-ekonomi. 18.12.1034].
25. Manon HS. ASMR mania, trigger-chasing, and the anxiety

of digital repletion. In: Basu Thakur G, Dickstein J, editors. Lacan and the Nonhuman. Palgrave Macmillan, Cham: The Palgrave Lacan Series; 2018. [Doi: 10.1007/9720188-3-319-63817-1_12].

26. Roberts N, Beath A, Boag S. A mixed-methods examination of autonomous sensory meridian response: Comparison to frisson. Conscious Cogn 2020;86:103046. [Doi: 10.1016/j.concog.2020.103046].
27. Yoon SJ, Park JE. Do sensory ad appeals influence brand attitude? J Bus Res 2012;11:1534-42. [Doi: 10.1016/j.jbusres. 2011.02.037].
28. Kalkan M, Odaci H. Gender and sex role in relation with attitudes toward seeking psychological help. Turk Psychol Couns Guid J 2005;23:57-64.
29. Kothari CR. Research Methodology: Methods and Techniques. Ansari Road, Daryaganj, New Delhi: New Age International (P) Ltd., Publishers; 2004.

ÜSKÜDAR UNIVERSITY

NP Medical Center
FENERYOLU - ETİLER

CHOOSE HEALTH

NP FENERYOLU MEDICAL CENTER

Adult Psychiatry Polyclinic
Child and Adolescent Psychiatry Polyclinic
Speech and Language Therapy Polyclinic
Occupational Therapy and Sensory Integration Clinic

NP ETİLER MEDICAL CENTER

Adult Psychiatry Polyclinic
Child and Adolescent Psychiatry Polyclinic

NP İSTANBUL Hospital

Feneryolu Medical Center Tel: +90 216 418 15 00
Etiler Medical Center Tel: +90 212 270 12 92

www.nptipmerkezi.com

nptipmerkezi NPİSTANBULBeyinHastanesi

ÜSKÜDAR UNIVERSITY

One more step in understanding human nature

www.uskudar.edu.tr facebook.com/uskudaruniversitesi twitter.com/uskudaruni

INDEX COPERNICUS INTERNATIONAL · J-Gate INDEXED · CiteFactor · TÜRKİYE ATIF DİZİNİ · BİBLIOMED · TÜRK PSİKİYATRİ DİZİNİ · ASOS indeks · OPEN ACCESS · TÜRK MEDLINE · Academic Resource Index ResearchBib · DRJI Directory of Research Journal Indexing · ROOTINDEXING JOURNAL ABSTRACTING AND INDEXING SERVICE